Titre: Title:	Consolidation Behavior Of Unidirectional Thermoplastic Composites Made From Glass Filaments (GF)/ Polyethylene Terephthalate (PET) DREF Yarns
Auteur: Author:	Natalia Cardona Vasquez
Date:	2023
Type:	Mémoire ou thèse / Dissertation or Thesis
Référence: Citation:	Cardona Vasquez, N. (2023). Consolidation Behavior Of Unidirectional Thermoplastic Composites Made From Glass Filaments (GF)/ Polyethylene Terephthalate (PET) DREF Yarns [Mémoire de maîtrise, Polytechnique Montréal]. PolyPublie. https://publications.polymtl.ca/10851/

URL de PolyPublie: PolyPublie URL:	https://publications.polymtl.ca/10851/
Directeurs de recherche: Advisors:	Louis Laberge Lebel, & Sampada Bodkhe
Programme: Program:	Génie mécanique

POLYTECHNIQUE MONTRÉAL

affiliée à l'Université de Montréal

Consolidation Behavior Of Unidirectional Thermoplastic Composites Made From Glass Filaments (GF)/ Polyethylene Terephthalate (PET) DREF Yarns

NATALIA CARDONA VASQUEZ

Département de génie mécanique

Mémoire présenté en vue de l'obtention diplôme du *Maîtrise ès sciences appliquées*

Génie mécanique

Mars 2023

POLYTECHNIQUE MONTRÉAL

affiliée à l'Université de Montréal

Ce mémoire intitulé :

Consolidation Behavior Of Unidirectional Thermoplastic Composites Made From Glass Filaments (GF)/ Polyethylene Terephthalate (PET) DREF Yarns

présenté par **Natalia CARDONA VASQUEZ**

en vue de l'obtention du diplôme de *Maîtrise ès sciences appliquées*

a été dûment accepté par le jury d'examen constitué de :

Eduardo RUIZ, président

Louis LABERGE LEBEL, membre et directeur de recherche

Sampada BODHKE, membre et codirectrice de recherche

Pascal HUBERT, membre

ACKNOWLEDGEMENTS

I would like to acknowledge in first place my family that were my support during this stage of learning. They were there to encourage and providing support when I was passing through difficulties with empathy and nonjudgmental, and always trusting in what I can do.

I also would like to acknowledge my supervisors, Louis Laberge Lebel and Sampada Bodkhe for providing the opportunity of participating in this project, and to open the doors to know this university that had provided a lot of knowledge as student as well as a person. Additionally, I would like to acknowledge Professor Myriam Brochu for providing priority to my experiences with the Acumen 12.

I want to acknowledge the technical support from Polytechnique for providing their ideas and their time to help me in developing the necessary tools to achieve the objectives of my research project. Especially Christian Charles Martel, Guy Gironne, Vincent Mayer, and Kambiz Chizari.

My acknowledgements to my colleagues at Polytechnique that helped me to get use to the laboratories and the general environment of the workspace.

I also acknowledge the members of the companies Filspec inc., BAUER, and Pultrusion technique, especially Martin Forest that was always there to answer my questions about the world of hybrid yarns and textiles processing.

I acknowledge PRIMA Quebec, NSERC, and the companies already mentioned for their financial support during my studies.

Finally, a special acknowledgement to Jeison for providing support, and for trying to get the best of every circumstance. I would not have probably arrived at this stage without his serenity.

RÉSUMÉ

Dans le contexte du développement de nouveaux matériaux composites avec moins d'impact environnemental, les composites thermoplastiques se sont imposés comme une alternative aux thermodurcissables. Cependant, la viscosité élevée des matériaux thermoplastiques a fait ses processus de fabrication plus complexe. Dans les méthodes de fabrication pour produire des composites thermoplastiques, les préimprégnés sont les matériaux predecesseurs les plus utilisés. Ils ont l'avantage de réduire l'effet de la viscosité élevée du polymère lors de la consolidation des composites. Néanmoins, les préimprégnés nécessitent une étape supplémentaire dans le processus de fabrication. L'utilisation de fils hybrides est présentée comme une opportunité pour réduire les distances entre le thermoplastique et les fibres de renfort, ce qui favorise leur imprégnation. La plupart des études ont utilisé et caractérisé des matériaux précurseurs de fibre mélangée, mais ils présentent l'inconvénient de l'endommagement des fibres de renfort lors de sa production, et aussi lors des opérations de fabrication ultérieures pendant sa consolidation. Les fils DREF apparaissent comme une alternative appropriée comme matériaux précurseurs des composites thermoplastiques. Ce type de fils hybrides présente l'avantage de protéger les fibres de renfort lors des opérations textiles en les recouvrant du polymère thermoplastique. De plus, comme le polymère crée un bouclier autour des fibres de renfort, il les protège lors du processus de consolidation, et il peut favoriser l'imprégnation de la phase de renfort en réduisant les distances thermoplastique – renfort. Les deux premiers objectifs de cette thèse consistent à développer des méthodologies pour préparer des préformes de fils thermoplastiques hybrides unidirectionnels, et à évaluer l'effet de la pression et de la température appliquées lors de la consolidation par moulage par compression. Les deux autres objectifs de cette thèse consistent à évaluer l'effet de la pression appliquée et de la température sur les caractéristiques finales de laminés unidirectionnels à partir de différents fils DREF de GF/PET. Les conclusions de l'étude soumise à la revue Composites Part A montrent la faisabilité d'utiliser des fils DREF comme matériel prédécesseur de composites thermoplastiques unidirectionnels, où des conditions de consolidation adéquates en pression et en température ont été déterminées pour atteindre l'épaisseur nominale pour les différents fils DREF évalués. Il a été possible d'obtenir des stratifiés consolidés avec des fractions volumiques de vides inférieures à 5 % et avec une résistance au cisaillement interlaminaire aussi élevée que 62 MPa en appliquant une pression de 492 kPa sous compression à 270 °C. De plus, il a été constaté que la torsion appliquée sur les fils DREF n'avait pas d'effet significatif sur les propriétés finales des laminés.

ABSTRACT

In the context of the development of new composite materials with a lower environmental impact, thermoplastic composites have emerged as an alternative to the thermosetting ones. However, the high viscosity of thermoplastic materials has difficulted the manufacturing process. Within the manufacturing methods to produce thermoplastic composites, prepregs are the most used precursor materials. They have the advantage of reducing the effect of the high viscosity of the polymer during the consolidation of the composites. Nevertheless, prepregs require an additional step in the manufacturing process. The use of hybrid yarns is presented as an opportunity to shorten the distances between the thermoplastic and the reinforcement fibers, and then to enhance their impregnation. Most of the studies have used and characterized hybrid yarns like commingled, but this type of precursor material presents the disadvantage of the damage that the reinforcement fibers undergo during production, and during the subsequent manufacturing operations during the consolidation. DREF yarns as a precursor material of thermoplastic composites emerges as a suitable alternative. This type of hybrid yarns has the advantage of protecting the reinforcement fibers during the textile operations by covering them with the thermoplastic polymer. Additionally, since the polymer forms a sheath around the reinforcement fibers, it protects them during the consolidation process, and it may enhancethe impregnation of the reinforcement phaseby reducing the thermoplastic – reinforcement distances. The first two objectives of this thesis consist in the development of the methodologies to prepare preforms of unidirectional hybrid thermoplastic yarns, and to evaluate the effect of the applied pressure and temperature during the consolidation by compression molding. The other two objectives of this thesis consist in the evaluation of the effect of applied pressure, and temperature on the final characteristics of unidirectional laminates from different GF/PET DREF yarns. The conclusions of the study submitted to the journal Composites Part A, show the feasibility of using DREF yarns as precursor material of unidirectional thermoplastic composites, where adequate consolidation conditions in pressure and temperature were determined to achieve the nominal thickness for the different DREF yarns evaluated. It was possible to obtain consolidated laminates with void volume fractions below 5 %, and with a short-beam strength as high as 62 MPa applying 492 kPa of pressure under compression at 270 °C. Additionally, it was found that the twist applied on the DREF yarns did not have a significant effect on the final properties of the laminates.

TABLE OF CONTENTS

LIST OF TABLES

LIST OF FIGURES

LIST OF SYMBOLS AND ABBREVIATIONS

Acronyms and abbreviations in English

ACFSlab	Advanced Composites and Fibre Structures laboratory
CMT	Compression Molding Tooling
DSC	Differential Scanning Calorimetry
ILSS	Interlaminar Shear Strength
GF	Glass Filaments
PA 6	Polyamide 6
PET	Polyethylene Terephthalate
PMC	Polymer Matrix Based Composites
T_g	Glass transition temperature
T_m	Melting temperature
TGA	Thermogravimetric Analysis
TPC	Thermoplastic Polymer Composites
TSC	Thermosetting Polymer Composites
UTM	Universal Testing Machine
V_v	Void Volume Fraction
V_F	Fiber Volume Fraction

LIST OF APPENDICES

CHAPTER 1 INTRODUCTION

A composite is constituted of mainly three components: (i) the matrix that corresponds to a continuous phase, (ii) a reinforcement that acts as the discontinuous phaseand is held by the matrix, and (iii) an interphase region that is created between the matrix and the reinforcement and facilitates the stress transfer from the matrix to the reinforcement. There exist a wide variety of matrices and reinforcements that can be used to produce a composite; however, polymer matrix-based composites (PMC) have earned a lot of interest. Their low density and remarkable mechanical properties composites have been the key to their success. By 1945 after their first peak, PMC industry have continuously growing and it is projected to grow at a CAGR of 10.1 % for the next 5 years [1].

Thermosetting polymer composites (TSC) were the first PMC developed for advanced composite industries such as aerospace and automobile [2]. Their three-dimensional cross-linked structure provides resistance to temperature and solvents; also, they allow high design flexibility, and they are more cost-effective [2]. Nevertheless, with the increasing demand of PMC, the reduction in production time has become a relevant factor [2]. For the latter, thermoplastic polymer composites (TPC) are considered an attractive alternative to TSC [2]. The cross-linked structure in TSC is obtained through chemical reactions, so, since in TPC there is not any chemical reaction, their manufacturing is directly limited by the heat transfer rate [2]. This means that processing temperature for TPC depend on thermal properties of the polymer matrix; once the dimensions of the TPC are achieved, it is usually cooled down below their glass transition temperature (T_g) [2].

Additionally, TPC can be remolded, they are recyclable, they allow reparation operations by welding, and they do not generate any toxic substances during the cross-linking process [3]. These are considered advantages compared to TSC [3]. However, TPC posses high viscosities (100 – 1000 Pa.s) and higher processing temperatures (130 °C – 400 °C) [3]. These are considered drawbacks because as higher is the viscosity, more difficult is to ensure that the thermoplastic polymer can easily travel within the composite, what is reflected as the ability of the polymer to wet or impregnate the reinforcement phase [2]. The understanding of how the thermoplastic nature in TPC affects the manufacturing and final properties of TPC been widely studied in the last years, but there still exist a lot of aspects that need to be covered, where pressure and temperature processing conditions are considered some of the most relevant [2].

To shorten the distances between the thermoplastic polymer and the reinforcement phase s to produce TPC, different types of hybrid yarns have been developed. A hybrid yarn is considered a technical yarn where reinforcing and matrix fibers are merged in one thread creating different structures or configurations that depend on the required characteristics of the final product [4]. Within the most used hybrid yarns in engineering, the commingled ones have been widely studied. They have demonstrated to have the potential to promote a homogeneous distribution of the fibers through the yarn cross-section what also allows a faster impregnation of the reinforcing fibers [5]. However, there are still drawbacks regarding commingling process linked to the damage of the fibers, and the fact that a large quantity of yarns cannot be produced effectively [6].

Core-sheath friction spun yarns like DREF (name attributed to its creator Dr. Emst Fehrer [7]) are produced by a friction spinning process where highly delivery rates (about 300 m/min) can be achieved. These yarns have the advantage of processing short or difficult handling fibers and to protect the reinforcement by covering it with the polymer that is in a spun form. This type of yarns has been already used in truck covers, canvas fabrics for military tents, and belts. However, there is still a lack of studies on the effect of manufacturing conditions that need to be performed to better understand the behaviour of DREF yarns when they are used to produce TPC [8].

In the context of a project funded by the Natural Sciences and Engineering Research Council (NSERC, RDCPJ 543847-19), and by PRIMA Quebec (R18-13-003); an Industry-Academia collaboration with the aim of obtaininga unidirectional low-cost TPC plates from DREF yarns was established. This project seeks out providing useful and sustained information about the use of DREF yarns as precursor material of unidirectional TPC. The principal objective of the present work is the study of the effect of temperature and pressure conditions on the final properties of unidirectional TPC made from glass filaments (GF) and Polyethylene terephthalate (PET) DREF yarns. To achieve this, a methodology to control the temperature and pressure during the consolidation of the TPC was developed. A L27 orthogonal Taguchi experimental design was used to select the combinations of temperature and pressure that were applied to GF/PET DREF yarns with different volume fractions, Tex, and twisting conditions. The final microstructure , the interlaminar shear strength (ILSS), and fracture surface were analyzed. This thesis includes a literature review to support the defined objectives followed by the proposed methodology and the submitted work for publication that includesthe obtained results and finishingwith the conclusions.

CHAPTER 2 LITTERATURE REVIEW

2.1 Technical textiles

Technical textiles are defined as textile materials and products that instead of being manufactured for aesthetic or decorative characteristics, are produced for their technical and performance properties [9]. Nowadays, the production of technical textiles from recycled polymeric materials is a pathway to decrease the environmental impact of plastic production where tens of millions of tons are disposed yearly. Recyclable thermoplastic polymers such as PET, polypropylene (PP), and polyamide (PA) have earned a lot of interest because of their economic value in the textile industry. However, PET fibres are considered by far the greatest synthetic fibre because of its strength, stiffness, and its ability to be tailored in very fine filaments [10].

2.2 Technical yarns

A yam is a continuous strand of filaments grouped in parallel (doubled) or twisted [11]. Technical yarns are produced to manufacture technical textiles. There are specific requirements for these yarns that depend on the intended end use, and it is directly related to the production techniques, raw materials selection and their combination [9].

2.3 Hybrid yarns as precursor material of polymer composites

Hybrid yarns are classified as technical yarns, and they have been used in the production of composites, where reinforcement and matrix fibres are combined to obtain a structure that is defined according to the final properties that are expected [9]. Initially, hybrid yarns were only used with thermoset matrices due to their low viscosity, and the ease to keep the architecture of the yarn during the processing. However, the use of thermoplastic hybrid yarns has earned a lot of interest, mainly because of their versatility, recyclability, welding characteristics, and toughness [3].

The use of hybrid yarns to produce TPC is focused on the development of architectures that enhances the shortening of the distances between the thermoplastic polymer and the reinforcement phases. Figure 2.1 shows a summary of the most common hybrid yams that are currently used for engineering applications and production of TPC.

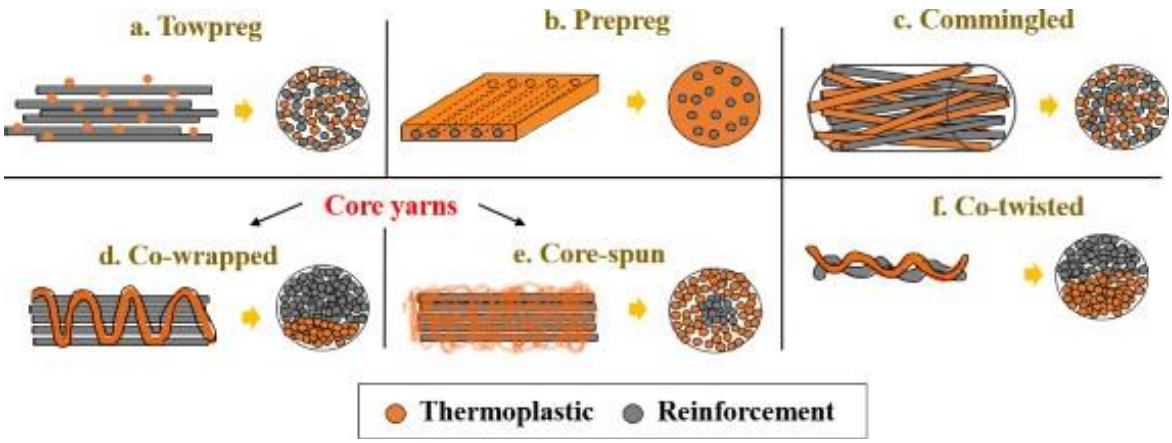

Figure 2.1. Schematic of the most representative thermoplastic hybrid yarns configurations: **a.** Towpreg, **b.** Prepreg, **c.** Commingled, **d.** Core-spun, **e.** Co-wrapped, **f.** Co-twisted

Towpregs and prepregs (Figure 2.1a and 2.1b) are basically preimpregnated systems consisting of reinforcing filaments impregnated with the thermoplastic polymer. They have the advantage of short polymer-reinforcement distances; however, a pre-heating is required before composite consolidation which usually increases the costs of the final products [12].

Commingled yarns (Figure 2.1c) are the result of the entanglements generated by air jet between the matrix and reinforcement filaments. The air impacts the two types of yarns orthogonally creating open segments where the reinforcement is exposed, and compact sections that are known as nips (present in both sides of an open segment) [13]. Adequate processing parameters such as pressure and speed are based on the minimization of filaments damage, and the homogeneous distribution of the components along the yam cross section [14]. Choi *et* al. demonstrated how the type of air-jet nozzle directly affects the arrangement of reinforcement filaments as well as the mechanical properties of the hybrid yam. They reported a decrease in damage of carbon filaments through surface treatments such as sizing; however, this alternative increased the adhesion that will have an impact on their uniform distribution [15].

Core yarns are composed of a compact agglomeration of reinforcement filaments enclosed by the polymer. Within this group, there exists co-wrapped hybrid yarns which are designed in a way that reinforcing filaments are surrounded by matrix filaments (Figure 2d) [16]. Wrap density (wraps of matrix filaments per meter) is an essential factor to consider for this configuration system, which will also depend on the structure of co-wrapped hybrid yarns resulting in meaningful effect on the

tensile properties [17]. Some authors have affirmed that as higher the wrap density is, better properties will be obtained for the composite [18]. This type of yarn has also been used in other structures like knitted and braided fabrics [19].

Core-spun yams are a combination of a reinforcing filaments called core which are enclosed by staple fibers. Staple refers to short filaments that are processed to reach a high degree of orientation [20]. The latter form a sheath, which will protect the core filaments from external adverse effects like damage friction during processing (Figure 2e). DREF core spinning is a friction spinning technology that has allowed the creation of high-performance core-spun yarns. In this open-end spinning system, the filaments are delivered in sliver form onto the carding drum surfacethat aligns and separate them. It is possible to obtain core-sheath hybrid yarns, where sheath filaments are attached to core filaments by a false twist that is generated by the rotation of the perforated spinning drums that brings the individual filaments together into the hybrid yam [21]. Figure 2.2 shows a schematic representation of friction DREF core spinning process.

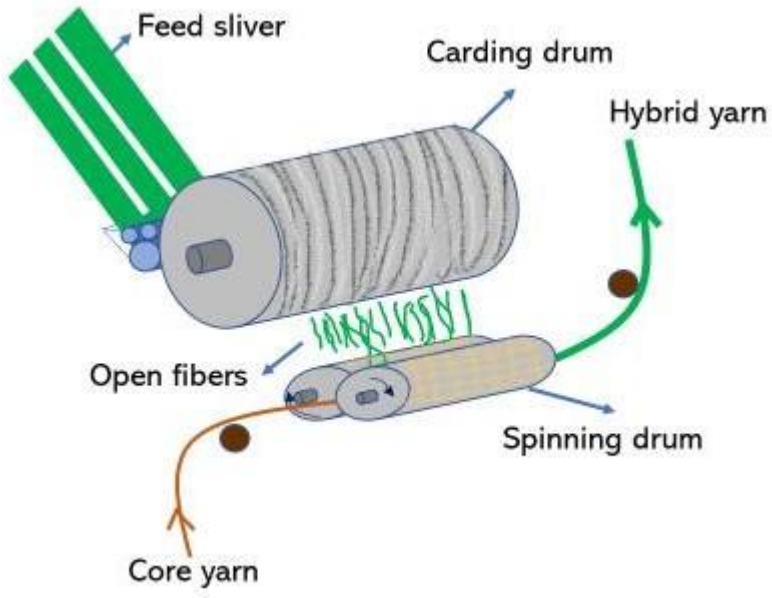

Figure 2.2. Schematic representation of DREF spinning process adapted from Bar et *al.* [22]

The twist is controlled by the rotation speed, but it cannot be measured; higher speed generates higher twisting on the DREF yam. It means that the control of the speeds in the drums is the way to obtain different empirical twisting levels [8]. The obtained yarn does not only have the advantage

of covering the continuous filament component like others core-spun systems, but also allows the introduction of the staples filaments (sheath) in the filament core, which provides an independent control of the core-sheath elements. This facilitates the combination and placement of different materials [7]. Since DREF friction spinning technology allows the control of the suction air pressure that affects the torque on the yarn [11], it may also enhance a higher compaction of the structure which is directly related to the capacity of the polymer to drape or impregnate the reinforcement [23]. A recent study of a DREF yarns made on the production of unidirectional composites (UD) from carbon fiber (CF) wastes and polyamide 6, demonstrated that it was possible to achieve at least 86 % of the strength of the CF filament heavy tow along with a high impregnation quality [23]. This shows the potential of using DREF yarns as a precursor material of TPCs; however, there is a lack of studies in the production of TPC that evaluated the final properties and characteristics for their composites.

2.4 Consolidation in thermoplastic composites

Consolidation refersto the stage of the manufacturing where heat and pressure are applied to obtain a monolithic structure, removing voids, and achieving a specific fiber volume fraction with the dimensional tolerances depending on the desired requirements [24]. Figure 2.3 shows a schematic representation of the thermal cycle for semicrystalline thermoplastic hybrid yarns when they are processed under heat and pressure. Glass transition temperature (T_g) is the temperature above which the amorphousregions of the polymer chains start to have mobility and the polymer becomes softer. Above the melting temperature (T_m) the order of the polymer chains is lost, and it transits to a viscous flow state. An overheating of the polymer above T_m to the degradation temperature (T_d) results in shortening of the polymer chains. Consolidation in thermoplastic manufacturing is a step where heat and pressure are applied to obtain a monolithic structure, without voids and/or volatiles [25]. It is important to clarify that all the temperatures (T_g, T_m, T_d) that are referred in the schematic represents the maximum value for each one when the material is heated up and cooled down. Also, the representation of the Pressure vs. Time diagram may vary from one manufacturing process to other. The slope and the segments that show the heating and cooling steps may also vary. They have only been drawn for a general representation of the stages during processing [26].

In Zone I the reinforcing and thermoplastic filaments are interacting only by physical contact at their interfaces; the position of the filaments is led by the configuration and design of the yarn. In the Zone II the polymer reaches its highest fluidity, which means that the viscosity plays a fundamental role regarding the distribution of the thermoplastic and the position of the reinforcing phase. Zone III corresponds to the consolidation process, the spaces where the polymer cannot flow into, will lead to void formation and decreasing of the composite mechanical properties. Finally, in Zone IV the consolidated composite is obtained. After consolidation, crystalline microstructure is formed in the thermoplastic. There are factors that affect the rate of crystallization such as the cooling rate and the polymer nature [26].

Table 2.1 presents different thermoplastic polymers and reinforcements used to produce TPC.

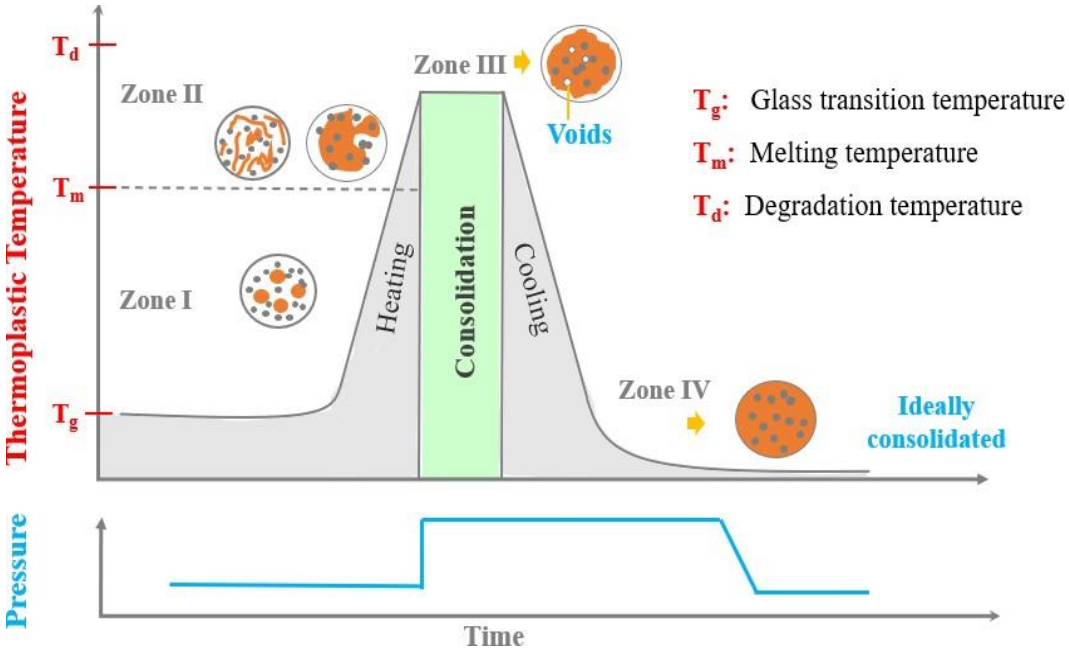

Figure 2.3. General thermal cycle for thermoplastic processing adapted from Wakeman et *al.* [26]

Table 2.1. List of some thermoplastic polymers and reinforcements that are use in the fabrication of TPC.

Material type		**References**
Thermoplastic Polymer	PA, PBT, PE, PEI, PEEK, PET, PMMA, POM, PP, PPS, PS, PSU, PVC	[27]–[29]
Reinforcement	GF, CF, Aramid	[30]–[32]

2.4.1 Consolidation methods used in the fabrication of TPC

The consolidation methods to fabricate thermoplastic composites are mainly based on the use of prepregs in automated techniques such as fibre placement and tape laying. In both the thermoplastics are softened at temperatures above T_g and pressureis applied. This allows the fusion of the plies that is generally achieved by discontinuous or continuous methods. First, the prepregs are stacked and then consolidated while they are in motion. Within the heat sources it is possible to find laser heating devices, microwave and ultrasonic systems, induction heating, and flame spraying. These techniques have the advantage of avoiding the consolidation in an autoclave [33]. Nevertheless, the use of autoclave is still valid regarding the final properties of the consolidated composites along with the possibility to obtain thicker samples [34].

In the case of consolidation of hybrid yarns to obtain TPC, there exist methods such as compression molding, filament winding, pultrusion, and autoclave molding. However, the first is by far the most relevant process in the industry for making structural TPC parts [35]. Compression molding has been also the onset for the study of the effect of pressure and temperatureduring the manufacturing of TPC from hybrid yarns, especially for unidirectional TPC, where the radial flow of the thermoplastic through the reinforcement filaments is assumed to be the predominant for their final impregnation [36].

2.4.2 Permeability in TPCs

Flow in composite reinforcements can be considered as f low of a fluid in a porous medium, described by Henry Darcy [37]. The Darcy's law for macroscopic flow can be with described by Equation ((2-1):

$$Q = \frac{-kA\Delta P}{\mu L} \tag{2-1}$$

where Q is the polymer flowrate (m^3/s), μ is the dynamic viscosity (Pa.s), k is the permeability (m^2), ΔP is the pressure drop across the porous media (Pa), A is the cross sectional area of the flow (m^2), and L is the length over which the pressure drop is taking place.

Permeability is a key parameter to understand the impregnation behavior and in the context of composites can be defined as the ability of a porous media of being impregnated by a fluid resin. Carman-Kozeny proposed an equation to calculate the permeability in any porous media through a relationship porosity and fiber radius [38]. The Carman-Kozeny principle can be expressed by Equation ((2-2):

$$k = [\frac{r^2}{4K}][\frac{\emptyset^3}{(1-\emptyset)^2}] \tag{2-2}$$

where the permeability (k) is the result of the ratio between the porosity ($\emptyset$), the particle radius (r), and the fitting constant (K), a.k.a the Kozeny constant. The Kozeny constant varies, and it needs to be measured experimentally due to the differences in the axial to the perpendicular flow [39]. This relationship does not consider any variation with time of the connectivity of a porous space, it means that the flow through a porous medium will be possible as long as the porosity is different from zero [40]. In the case DREF hybrid yarns there is not still a rigorous study that characterizes the permeability parameter for flow along the cross-section of the reinforcement core.

Other authors like Gutowski *et al*. proposed a modification of the Carman-Kozeny equation for flow transverse to reinforcement filaments, where the locking generated within the filaments due

to compression forces during consolidation generates changes in pressure and for instance in the permeability [39]. The Gutowski principle can be expressed by Equation (2-3):

$$k = \frac{r^2 \left[\frac{V_a}{V_f} - 1\right]^3}{4K \left[\frac{V_a}{V_f} + 1\right]} \tag{2-3}$$

where V_a is the volume fraction at which the bed made from filaments becomes impermeable, V_f is the volume fraction of the reinforcement filaments, K is the Kozeny constant, r is the fiber radius [41].

2.4.3 Developments in tracking methods during consolidation of TPCs

Tracking of the evolution of variables during consolidation of TPCs such as thickness, deformation of reinforcement filaments or mats, and pressure is still challenging in composites industry [34]. This is explained by the sensitivity of these variables on the manufacturing conditions, and the complexity for the development of systems that are able to accurately track them during all the consolidation process [34]. Modeling have been used by several researchers to try to estimate the changes that occur with every constituent of TPCs during consolidation. Michaud et *al.* developed a model to predict the impregnation and the evolution of fiber volume fraction while the resin front passed through the fiber mat [42]. This model was used afterwards by the same authors to be used with an industrial relevant thermoplastic polymer such as polypropylene (PP) [43], and they could demonstrate that even using the predictions from the proposed model, the high viscosity of the PP, along with the mat structure, and the way how pressure is applied (one-step, or two-steps) could significantly affect the accuracy of the results for small size samples. Murtagh et *al.* [44] focused in the development of a system to evaluate the flow mechanisms involved in consolidation of TPCs by using pressure and Linear Variable Differential Transformer (LVDT) transducers. Figure 2.4 presents the consolidation apparatus used by them. Using this system, the authors were able to track the changes in force, polymer flow, and thickness during consolidation of a TPCs with a PEEK as polymer. The authors stated that the proposed analysis will allow manufacturers to specify consolidation and forming parameters to produce parts with higher quality, where fiber buckling,

void formation, and delamination could be prevented. However, none of the latter variables were characterized to be linked with the obtained results, and no more additional works using the same system were reported by these authors.

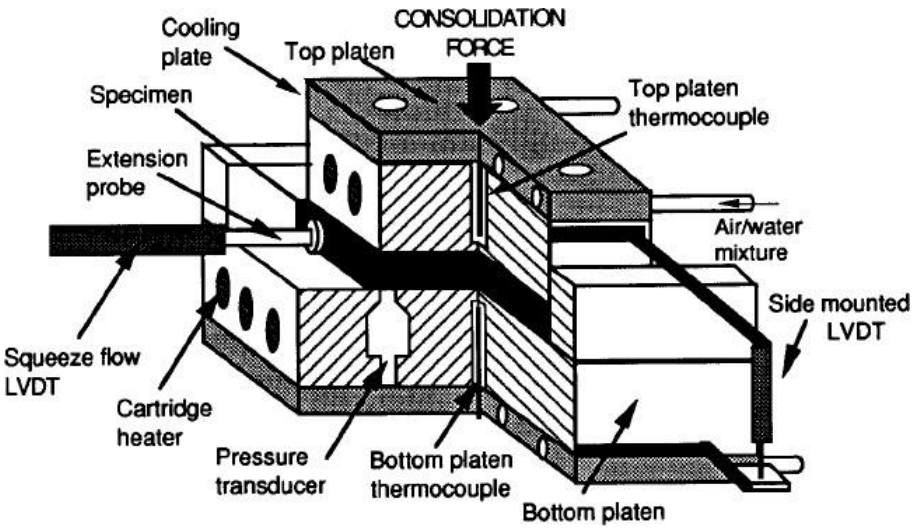

Figure 2.4. Consolidation apparatus developed by Murtagh et *al.* [44]

Hautefeille et *al.* [45] developed a compression molding system equipped with a UV detector that was able to track the position of the fiber tows of a woven fabric when a low-viscosity fluid was introduced by pressure through compression. They evaluated fluid with viscosities from 0.02 to 9.65 Pa.s founding that the fibers motion is more remarkable as the fluid-solid stress increases. Also, they reported how the fabric architecture influenced the fluid flow, an example of this is the restricted flow in the weft direction due to its lower permeability if it is compared with the wrap one. They also reported that the fiber-tows washout started at the beginning of the compression where it was not possible to balance the force that the fluid exerted on the fibers (i.e drag force). Washout refers to the displacement of the fibers due to the shear stresses that are generated between the resin and the fibers. Figure 2.5 shows the system developed and employed by Hautefeuille et *al.*

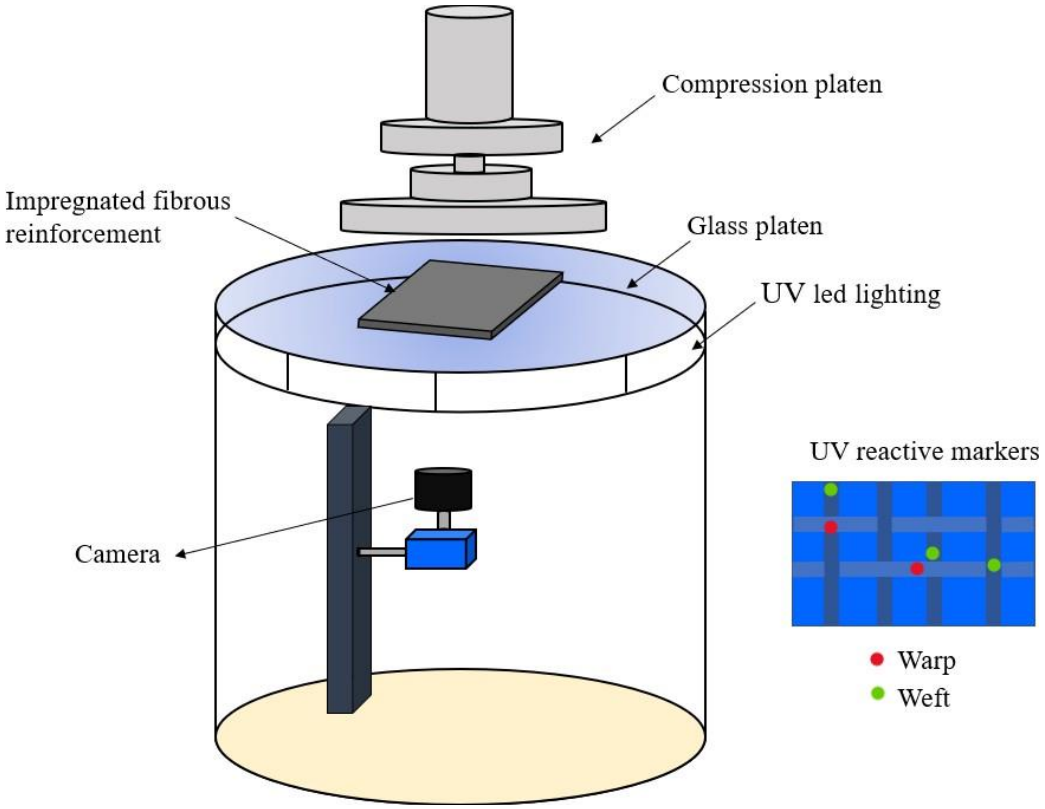

Figure 2.5. In-plane flow visualization setup to track fibers position during compression adapted from Hautefeuille et *al.* [45]

The same authors reported above employed the system shown in Figure 2.5 to evaluate a different fabric corresponding to a quasi-unidirectional weft fabric. Their main objective was to propose a generic method to measure the deformation fields of different reinforcement, and to identify the driving forces that generated the fibers washout [46]. They were able to identify and localize the fiber tow deformation when the fabricwas under compression which provides relevant information to understand the in-plane deformation of the fibers. To track the in-plane (x,y) displacement during the application of compressive pressures, they used the algorithm proposed in [45] by identifying an initial reference point for each tow that was constantly tracked by using UV-reactive markers. With the obtained results, the authors found that once the fabric is under compression, it undergoes local non-homogeneous in-plane deformations. These deformations propagate transversely in the fiber tows of the fabric creating a 'barrelling' effect where the edges of the fabric start to evidence the deformation and it is gradually passed to the center of the fabric.

Both studies reported by Hautefeuille et *al.* have exposed a methodology focused on the understanding of the fiber displacements and the drag forces that a fluid exerts when a fabric is under compression. Nevertheless, since the viscosities of the fluids they tested are very low compared to the ones for a thermoplastic matrix (20 – 200 times higher aprox.), it is relevant to evaluate if the behaviour of the fabric that would be used as reinforcement in the case of the production of TPCs would present the same patterns, and if the modeling is able to accurately predict the position and the drag forces that the thermoplastic matrix would generate within the fibers. Additionally, the study of unidirectional fabrics and the consolidation of hybrid yarns such as DREF has not been reported.

2.5 Characterization techniques for TPCs

Within the essential requirements in developing composites materials there exist a special interest in the proper understanding of the relationship between the final properties and characteristics of the composite with its composition and structure. To achieve this there are mainly two groups for the characterization of composites. One refers to the analysis of the microstructure and the other seeks for the evaluation of the mechanical properties [47]. Nevertheless, there are also other characterization techniques that are used to determine the thermal properties of the polymer that will lead the determination of processing conditions of the TPC such as thermogravimetric analysis (TGA) and differential scanning calorimetry (DSC). With TGA it is possible to know the changes in weight of the material as the temperature is increased, this technique is helpful to determine degradation temperatures of the polymer as well as the presence of mineral charges. DSC is used to determine the T_g, T_m and crystallization temperature (T_c) [48].

2.5.1 Microstructure characterization

The relevance of the microstructure in defining the properties of TPCs is well known [37][39][40]. Since the final microstructure is highly influenced by the processing conditions, the understanding of the widely varying properties obtained for the same material processed in different ways has opened the door for the development of techniques to characterize the microstructure. However, in the case of PMCs, there exists a complexity related to the great amount of reinforcement and polymer types. For example, the use fabrics created by weaving, knitting, and braiding has

contributed to the creation of complex reinforcement geometries in all three dimensions. Aside from the changes that the reinforcement transits during processing where the compression applied during consolidation and the polymer flow are essential in optimizing the process to minimize voids and to achieve a proper reinforcement wetting or impregnation [47].

Voids are considered one of the most important criteria to determine the quality of the fiber-reinforced composites due to their effect on the final mechanical performance [51]. Macro and micro voids are the most common types of this defect present in the microstructure of polymer composites [52]. Both are mainly generated by the air entrapment in highly viscous polymers, with the difference that macro voids can be easily appreciated with naked eye while micro voids are formed within the filaments of the yam, which implies the use of specialized optical microscopes for its observation [53]. Optical and electron microscopies are two of the most recognized techniques to characterize the microstructure of polymer composites. Both techniques allow the observation of the morphology, constituents, and fracture surfaces; however, they are usually employed as techniques that complement each other [54]. The main difference between optical and electron technologies is the beam applied to the sample, where the former uses light and the latter applies electrons beams [54]. This means that electron microscopy technique can provide high-resolution images and more accurate characterization of the topography of the sample compared with optical techniques, what is also the reason of using electron technologies in the analysis of fracture surfaces [55].

Image analysis and image processing techniques are also used to characterize the microstructure of TPCs [54]. The main objective of these techniques is the quantitative analysis of the phases, features, and structures present in the consolidated TPCs [54]. Nevertheless, the fact that both are considered as advanced techniques implies the use of high-performance equipment, which is considered a disadvantage because of their cost [56]. Another drawback is the time required to select an accurate method within the wide range of possibilities [56]. Quantification of the composite constituents can be then assessed by optical and image processing techniques; however, since the image thresholding is very sensitive to the imaging conditions, it implies a high inversion of time in their parameterization [57]. In this case, density-based methods such as acid digestion or matrix burn-off are considered a reasonable option based on their cost-accuracy ratio [57].

2.5.2 Mechanical characterization

Evaluation of mechanical properties in composites are used as a mean to characterize the performance of it when it is under specific conditions. In this evaluation converge numerous experiments that are designed to verify its basic features. There are standardized tests to study the mechanical behavior of the composites such as friction, impact, tensile, compression, and flexural tests. However, the criteria for the selection of the mechanical test depends on the information is expected to provide. In the case of TPCs as mentioned in 2.5.1, voids are usually considered defects. A matrix-dominated properties such as the interlaminar shear strength (ILSS) serves as an adequate mechanical testing technique due to its intimate dependence on the void volume fraction (V_v), where ILSS tends to decrease as V_v increases [58][59]. ILSS is also considered a relevant indicator to measure the interfacial adhesion between the reinforcing fibers and the polymer matrix, where high values of ILSS are related to better interfacial adhesion [60]. The formation and evolution of voids in the consolidation of TPCs are linked to the differences in thermodynamic and rheological phenomena as well as the deformation of the reinforcement fiber during the application of the pressure [24][61]. Besides the properties of the polymer, the permeability of the reinforcement is another predominant factor to achieve the best performance in the mechanical properties of the composites. Permeability can be defined as a measure of the ease with which a porous media can be impregnated by a fluid resin [62].

CHAPTER 3 ORGANIZATION OF THE RESEARCH AND RESEARCH OBJECTIVES

3.1 Problem statement

According to the literature review it was possible to identify some gaps in the study of the consolidation behavior of hybrid yarns like DREF as precursor material of unidirectional TPCs. It was found that most of the works focused on the evaluation of TPCs from fabrics made of commingled yarns. Additionally, the use of carbon fibers was predominant as reinforcement phase. Thermoplastic matrices included the use of polyamides, or polyarylether ketones such as PolyEther Ether Ketone (PEEK). Ono *et al.* studied the final properties of TPCs from woven commingled yarns made of carbon fibers and nylon [63]. Long *et al.* studied the mechanical properties of unidirectional TPCs from commingled yarns discussing the mechanism of impregnation of the polypropylene matrix within the glass fibers [64]; however, the methodology to ensure the alignment of the yarns is not yet clear. Hasan *et al.* developed a unidirectional TPC from polyamide/carbon fibers DREF yarns obtaining at least 86 percentage of the tensile strength of composites from virgin carbon fibers yarns [23]. These studies do not consider matrices as polyethylene terephthalate that corresponds to one of the most important commodity thermoplastic polymer, and the use of glass fibers that is the most used reinforcement used in the fabrication of PMCs [65]. Additionally, the consolidation parameters for the use of DREF yarns to produce TPCs need to be explored.

In the framework of the industrial – academia collaboration project funded by the Natural Sciences and Engineering Research Council (NSERC, RDCPJ 543847 -19), and by PRIMA Quebec (R18-13-003), the study of the consolidation behavior of unidirectional TPCs from GF/PET DREF yarns, and the evaluation of the final properties of the laminates were established.

3.2 Research objectives

Objective 1: To develop a methodology to prepare preforms of unidirectional hybrid thermoplastic yarns. A winding method to ensure the alignment of hybrid thermoplastic yarns was developed. A custom sample holder was used to wind the yarns and to achieve the same final

tension. The parameters for winding to ensure an adequate comparison between the wound yarns were verified.

Objective 2: To develop a new methodology to control the applied pressure and to evaluate the thickness evolution during the consolidation of thermoplastic composites from hybrid yarns. A custom compression molding tooling was adapted to a universal testing machine equipped with a laser extensometer. The pressures were controlled through the load cell, and the thickness evolution for each sample was tested by using the extensometer.

Objective 3: To determine the effect of pressure and temperature on the final thickness, microstructure, and mechanical properties of consolidated composites from GF/PET DREF yarns. A custom controller was used to heat the compression molding tooling. To avoid interference with the data acquisition of the load cell, a cooling system was adapted to the tooling. Material, temperature, and pressure were defined as the factors for the experimental design that was based on a Taguchi L27 orthogonal array. Different pressures and temperatures were applied to the wound preform according to interactions defined by the Taguchi design. Samples from the consolidated plates were cut to evaluate the microstructure and the short-beam strength of the obtained TPCs.

Objective 4: To determine the effect of the Tex of the filaments, twisting, and non-twisting conditions on the microstructure, and mechanical properties of consolidated composites from GF/PET DREF yarns. A statistical analysis of the results was used as the basis to determine the effect of the materials' characteristics in the obtained properties for the consolidated composites. For this Minitab software was employed.

3.2.1 Article that covers the research objectives

All the objectives presented in this thesis are presented in the form of an article submitted to the journal, *Journal of Composite Materials.*

CHAPTER 4 ARTICLE I: CONSOLIDATION OF DREF YARNS PRECURSOR FOR MANUFACTURING GLASS-FIBER POLYETHYLENE TEREPHTHALATE THERMOPLASTIC COMPOSITES

Natalia Cardona, Sampada Bodkhe, Louis Laberge-Lebel. Journal of Composite Materials. JCM-23-0372. Submitted on April 5th, 2023.

Abstract

Unidirectional composite laminates of glass fiber (GF)/polyethylene terephthalate (PET) from DREF yarns with different volume fractions, linear density, and twisting conditions were obtained by compression molding. A compression molding tooling was designed and adapted to a universal testing machine equipped with a laser extensometer. Consolidation pressures between 98 and 492 kPa, and temperatures between 260 and 280 °C were applied. The combination of the test conditions was defined according to a Taguchi orthogonal array. The consolidation behavior was analyzed based on the study of the evolution in pressure and thickness of the samples with time. The nominal thickness for all the laminates was calculated and compared to establish the required conditions of pressure for each DREF type. Laminates with void volume fractions lower than 5 % and with an interlaminar shear strength as high as 62 MPa were obtained. Fracture surfaces of the laminates showed differences such as the presence unimpregnated GFs in the delamination of highly and poorly impregnated laminates. The statistical analysis demonstrated the applied twist did not have a significant impact on the properties of the obtained laminates. The results obtained support that hybrid yarns such as DREF are suitable for the use as precursor material of thermoplastic composites.

4.1 Introduction

Thermoplastic composites (TPCs) are recyclable, can be remolded, welded for assembly or reparations and are known for their high toughness [66]. However, unlike thermosetting polymers used traditionally in composite applications, thermoplastic polymers present high viscosities (100 – 1000 Pa.s [3]), and require high processing temperatures (130 – 400 °C [3]). This fact along with

the still evolving technologies for the production of TPCs have limited the implementation of these materials at industrial scale [67].

Reinforced thermoplastic hybrid yarns have emerged as a suitable solution to create an intimate contact between the polymer and the reinforcement and counter the effect of high viscosities [68]. A yarn is a group of continuous filaments assembled in parallel, that may or may not be subsequently twisted together. [11]. Filaments of reinforcement and polymer matrix create a 'hybrid' that can be processed to obtain a composite material. DREF yarns consist of a continuous fiber core onto which discontinuous polymer fibers are spun using the friction spinning process [69]. In thermoplastic composites, the core can be made of continuous reinforcement filaments covered by spun fibers made from the polymer matrix [11]. DREF yarns have the advantage of the protection of the reinforcement during transport and handling, which is less achievable with other more common hybrid yarns like commingled. In commingled yarns, the polymer filaments are intermixed with the reinforcement, so, a part of the surface of the reinforcement is directly exposed to the processing media [15]. DREF yarns can be twisted or untwisted. Untwisted condition is referred to a textile process where several yarns are combined together and then wound in parallel to form a larger yarn [70]. Untwisted yarns can be twisted together clockwise or counter clockwise with a certain number of rotations per unit of length [71].

Another benefit of using DREF yarns is the flexibility to tailor the core to sheath ratio, and the possibility to obtain high production rates (up to 250 m/min) [11]. Through DREF spinning, it is possible to obtain higher compaction of the structure which is directly related to the capacity of the polymer to drape or impregnate the reinforcement [23]. A recent study of DREF yarns made on the production of unidirectional composites (UD) from carbon fibers (CF) wastes and polyamide 6, demonstrated that it was possible to achieve at least 86 % of the strength of the CF filament heavy tow along with a high impregnation quality [23]. This study showed the potential of using DREF yarns as a precursor material of TPCs. However, the use of other widely common polymers used in the textile industry such as Polyethylene Terephthalate (PET) and reinforcements such as glass fibers (GF) is still unexplored.

During consolidation, heat and pressure is applied to obtain a monolithic structure, removing voids, and achieving a specific thickness and fiber volume fraction [24]. Voids are considered one of the

most important criteria to determine the quality of the fiber-reinforced composites due to their effect on the final mechanical performance [51]. Matrix-dominated properties such as the interlaminar shear strength (ILSS) has an intimate dependence on the void volume fraction (V_v), where ILSS tends to decrease as V_v increases [58][59].

Mathematical modelling is an option to understand and accurately evaluate the most predominant factors in the consolidation of composites including their permeability [72]. However, since most of the material characterization (e.g. rheological experiments of the polymer [36], reinforcement compaction behavior [73]) that sustains the validation of the models is performed on individual components, the interaction mechanisms like impregnation cannot be always described by the constituents separately [74]. Valverde et *al.* [75] presented a methodology based on compression experiments to characterize the behavior of TPCs under rapid processing conditions including the modelling of the evolution in thickness and width. They evaluated preconsolidated (made in autoclave at 320 °C and applying 7.0 bars of pressure) and non-preconsolidated samples and found a high dependence of the thickness evolution with temperature. However, once the experimental results were compared with those obtained from the developed model, it was observed that the thickness was accurately predicted whilst the width was not. Additionally, the effect of the thermal history of the preconsolidated samples on the obtained results was not clear, which may be relevant considering the possible changes in crystallinity that temperature and cooling rates could have induced. This demonstrates there are still challenges to address when mathematical modelling is used to understand the consolidation behavior of TPCs.

Hautefeuille et *al.* proposed in a recent study [76] a methodology to dynamically measure the changes in force and position of the fiber tows during consolidation by compression molding. These changes were generated by the deformation that the fluid induced within the fiber tow of a weft fabric. They demonstrated that the drag force produced by a silicon fluid is greater that the form drag that is mainly dependent on the shape of the fabric. Measurements of the thickness was achieved by developing an algorithm based on tracing and registration techniques that included the use of optical system that detected an UV markers patterns set previous the consolidation. Even if this study presents a robust experimental methodology, it is still unclear if the behavior of thermoplastic polymers with a viscosity 20 times greater than the silicon could be accurately predicted and modeled.

On the other hand, the required characterization techniques to evaluate the properties of the composites after consolidation also play an important role. Optical and electron microscopy are two of the most recognized techniques to characterize the microstructure of polymer composites. Both techniques allow the observation of the morphology, constituents, and fracture surfa ces; however, they are usually employed as techniques that complement each other due to their resolution and magnification features [54]. Quantification of the composite constituents can be then assessed by optical and image processing techniques; however, since the image threshold is very sensitive to the imaging conditions, it implies a high investment of time in their parameterization [57]. In this case, density-based methods such as acid digestion or matrix burn-off are considered a reasonable option based on their cost-accuracy ratio [57].

The aim of this study is to evaluate the consolidation behaviour of different DREF precursor yarns for GF/PET TPCs through the implementation of a methodology that allows to control the applied pressure, the alignment of the GFs, and the temperature. The microstructure of the consolidated samples was analyzed by optical microscopy; the ILSS for each group of samples was obtained and the fracture surface was observed by SEM microscopy.

4.2 Experimental section

4.2.1 DREF yarns

The yarn materials were S2-Glass (GF) (933, AGY, density = 2.46 g/cm^3) and Polyethylene terephthalate (PET, density = 1.43 g/cc) (staple fiber, Huvis Corporation). The yarns were obtained by DREF friction spinning (FilSpec Inc.). PET staple fibers completely enclosed the glass fibers core to obtain a GF/PET DREF tow. Then, eight tows were combined into yarns with or without twist. A total of three types of DREF yarns were evaluated: M1, M2, and M3. Their main characteristics are presented in Table 4.1. M1 was made with a finer glass fiber core of 22 Tex; this glass fiber core was composed of 200 filaments of 7 µm in diameter which was overspun by 13.3 Tex of PET fibers. The resulting fiber volume fraction (V_f) of the DREF tow was 52.2%. M2 and M3 were made using a larger glass fiber core of 66.6 Tex. For M2 and M3, the glass fiber core was composed of approximately 408 filaments of 9 µm in diameter. The cores were overspun with approximately 27 Tex of PET fibers. The resulting V_f was 60%. Tex of PET may vary throughout

the yarn's length. To obtain a reference value, the Tex for the PET in the yarns were measured with a precision scale (ME103TE, Mettler Toledo). The cross-sectional areas (A) of the glass (f) and PET (m) components of the yarns were determined by,

$$A_{(f,m)} = \frac{F_{(f,m)}}{1000 \cdot \rho_{(f,m)}} \tag{4-1}$$

where F is the linear density in Tex, and ρ the density in g/cm^3. After combining the eight tows together, no twist was applied to M1 and M2 while M3 was twisted in a S configuration with 20 turn per meter. The total cross-sectional material area in each yarn (A_Y) was calculated by,

$$A_Y = 8\ ^{tows}/_{yarn} \cdot (A_f + A_m) \tag{4-2}$$

where A_f and A_m are obtained from Eq. (4-1).

Table 4.1. Tex (g/1000 m), volume fractions, number of tows bundled, twisting and non-twisting conditions for the three materials made of GF/PET DREF yarns used in this study.

DREF yarns	Tex in one tow (g/1000 m)		Volume Fractions (V_{GF}/V_{PET})	Number of bundled tows/yarn	Cross-sectional area of material per yarn (mm^2)	Twist
	GF	PET				
M1	22.0	13.3 ± 1.7	52.2/47.8	8	0.15	No
M2	66.0	27.4 ± 0.3	60/40	8	0.37	No
M3	66.0	27.3 ± 0.3	60/40	8	0.37	Yes

Figure 4.1 shows an illustration of the cross-section and longitudinal views of the DREF yarns used, followed by their micrographswhich were taken with a microscope (VHX700, Keyence. One DREF yarn consists in a bundle of eight tows made of glass filaments enclosed by spun PET polymer. It is observed that the yarns of M1 are thinner than the ones of M2 and M3 due to the difference in Tex, i.e., 22 for M1 and 66 for M2, and for the difference in the volume fractions. Additionally, even if M2 and M3 had the same Tex, the twisting applied to M3 increased the compaction between yarns.

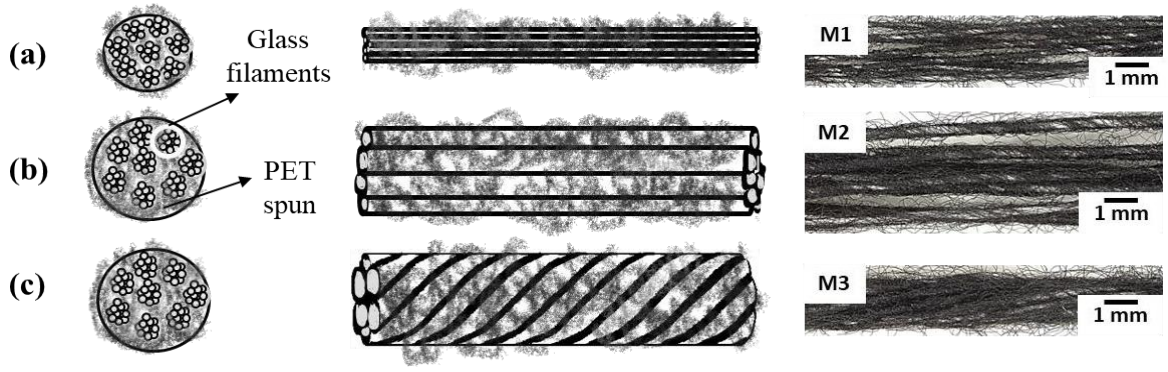

Figure 4.1. Illustration of cross-sectionand longitudinal view of a DREF yarns used in this study, and micrographs of the DREF yarns ‘as received’ for (a) M1, (b) M2, (c) M3

4.2.2 Compression molding experiments

Figure 4.2 shows the steps for compression molding experiments of GF/PET DREF yarns. Figure 4.2(a) shows the ‘as received’ bobbin with DREF yarns. The M1, M2, and M3 materials all had similar packaging.

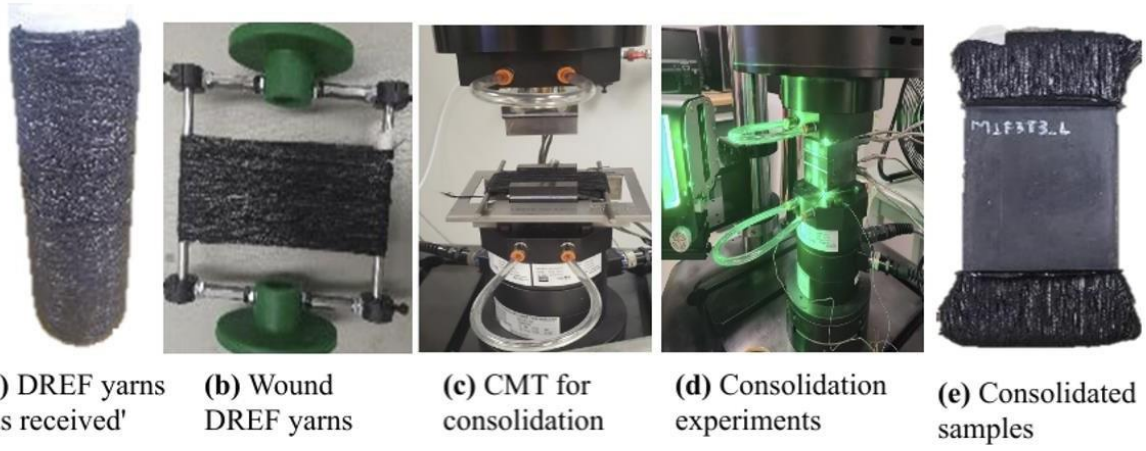

Figure 4.2. Process steps for compression molding of GF/PET DREF yarns: **(a)** DREF yarns in a bobbin 'as received'; **(b)** Wound DREF yarns with unidirectional arrangement; **(c)** Concave (upper) die and convex (bottom) die of CMT for consolidation with DREF yarns placed in the convex die; **(d)** Assembly for consolidation experiments in the UTM with the laser extensometer, and **(e)** Consolidated samples

Figure 4.2(b) shows the rectangular winding apparatus holding two stainless steel rods separated by 90 mm. The fixture was placed in a computer-controlled winding apparatus equipped with a yarn feed point on a linear actuator. A yarn was fixed to one of the rods using pressure sensitive tape. The winding apparatus was then rotated keeping the tension in the yams at 2.1 N. During rotation the yarn feed point was moved back and forth by a linear distance of 40 mm. The linear moving speed of the yarn feed point was adjusted to depose yams side-by-side on the winding apparatus without overlap. When the yarn feed point reached the end of the 40 mm distance, the feed point moving direction was inversed to wind the next layer. The winding parameters were adjusted to reach approximately 15 g of wound material. Figure 4.2(c) shows a DREF material wound onto the winding apparatus. The total cross-sectional area of the wound material can be calculated according to,

$$A_C = A_Y \cdot N_W \cdot 2 \qquad 4\text{-}3$$

Where the A_Y taken from Eq. (4-2) is multiplied by the number of windings (N_w) and a factor of 2 yarns per winding.

The wound material onto the two rods were transferred into a spring-loaded sample holder keeping the tension in yarns at approximately 2.1 N. Figure 1(d) shows the sample holder and material placed into the convex die (bottom) of a compression molding tool (CMT, AISI 4140 steel, total volume = 40 x 50 x 15 mm^3). Figure 4.2(d) also shows that the CMT installed in a Universal Testing Machine (UTM) (Acumen 12, MTS) coupled with an independent cooling system to avoid any interference with the data acquisition of the load cell. The consolidation pressure was controlled by the UTM. The distance between the convex and concave dies was acquired using a laser extensometer AOX (Advantage Optical Extensometer, MTS, accuracy = 1 - 5 µm) tracking the position of white parallel lines engraved on the dies. This measurement system ensured that the compliance of the tooling and UTS assembly did not interfere with the tracking of the consolidation thickness. The nominal consolidated thickness could be calculated using,

$$T_{th} = \frac{A_C}{tool\ width} \tag{4-4}$$

Table 4.2. presents the values of number of windings (N_W), A_C, and T_{th} obtained for M1, M2, and M3.

Table 4.2. Number of windings (N_W), cross-sectional area of the wound material (A_C), and the nominal consolidated thickness (T_{th}) for M1, M2, and M3.

DREF yarns	N_W	A_C (mm^2)	T_{th} (mm)
M1	256	75.3	1.88
M2	147	107.4	2.69
M3	148	108.7	2.72

Before every consolidation experiment, the CMT was heated until it reached the desired temperature. Subsequently, the yarns' sample holder with the wound DREF yarns were placed into the CMT cavity, the laser extensometer was tared, the force was applied and held constant for 4 min. and then the mold was cooled down until the CMT cavity reached 60 °C to proceed with the demoulding of the consolidated sample.

4.2.3 Taguchi orthogonal array experimental design

Consolidation conditions were defined based on a Taguchi orthogonal array experimental design [77]. Material, temperature, and applied pressure were defined as the test factors, each one with three levels. Molding temperatures between 260 and 280 °C were used. Pressures between 98 and 492 kPa were applied. Table 4.3 shows the 9 different parameter combinations tested. A total of three replicates for each test condition were evaluated. One - way ANOVA with significance level of 5 %, and the interaction between the test factors were evaluated with a statistic software (Minitab) to determine the existence of significant differences between them.

Table 4.3. Taguchi orthogonal array experimental design, factors, and their interactions.

DREF yarns	Applied force (kN)	Equivalent pressure (kPa)	Temperature (°C)	Sample name
M1	0.2	98	260	M1P1T1
	0.6	295	270	M1P2T2
	1.0	492	280	M1P3T3
M2	0.2	98	270	M2P1T2
	0.6	295	280	M2P2T3
	1.0	492	260	M2P3T1
M3	0.2	98	280	M3P1T3
	0.6	295	260	M3P2T1
	1.0	492	270	M3P3T2

4.2.4 Characterization

Modulated Differential Scanning Calorimetry (MDSC 2000, TA instruments) were performed on PET samples (average weight ~12 mg), with a nitrogen (N_2) atmosphere at a flow rate 50 ml min^{-1}. A modulation amplitude of 0.5 °C/min, with a period of 40 s, and heating rate of 5 °C/min were

applied to determine the glass transition (T_g), melting (T_m), and recrystallization (T_c) temperatures. Second heating runs in DSC to erase the thermal history of the polymer were not applied since the material was used for consolidation experiments 'as received'. Degradation temperature (T_d) was determined by Thermogravimetric Analysis (TGA Q500, TA instruments). The test was performed on PET samples of ~12 mg with N_2 and air as carriers with the same flow rate mentioned in MDSC between 40 to 600 °C at a heating rate of 5 °C/min.

The consolidated sample GF's and PET's volume fractions (V_F, V_{PET}) were measured by ignition method according to the procedure G of ASTM D3171-99, using nominal material densities. Void volume fraction (V_v) was determined according to ASTM 2734. The actual density of the consolidated samples was measured using the Archimedes method per ASTM D792.

Specimens were cut from the cross section of the consolidated laminates and embedded in epoxy resin for microscopic analyses. The embedded specimens were polished using an automatic surface preparation machine (Tegramin 25, Struers). Polished surfaces were observed at different magnifications under optical microscope (VHX700, Keyence) using a of brightness 270 cd/m^2, and contrast ratio 450:1.

The interlaminar shear strength (ILSS) was tested by short-beam strength method in a UTM (Insight, MTS). The specimens to be tested were cut from the consolidated samples with a width to thickness ratio of 2:1, and a span length to thickness ratio of 6:1 in compliance with ASTM D2344. The specimens were loaded at a 1 mm/min.

The morphology of the fracture surface of the specimens tested in by short beam method were observed using a Scanning Electron Microscope (SEM, TM3030, Hitachi). Fracture surface was coated with a thin layer of gold using an automatic sputter prior to the observation by SEM. The sputter environment was argon gas.

4.3 Results and discussion

4.3.1 Thermal properties obtained from TGA and MDSC

TGA and MDSC curves obtained for the PET taken from GF/PET DREF yarns are presented in Figure 4.3 and the thermal properties in. All the values obtained for T_g, T_m, T_c, and T_d, are within

the ranges commonly reported for PET [78]–[80]. This study does not cover the characterization and the effect of low molecular weight compounds added during the manufacturing of the PET or the presence of moisture from hygroscopic nature of this polymer.

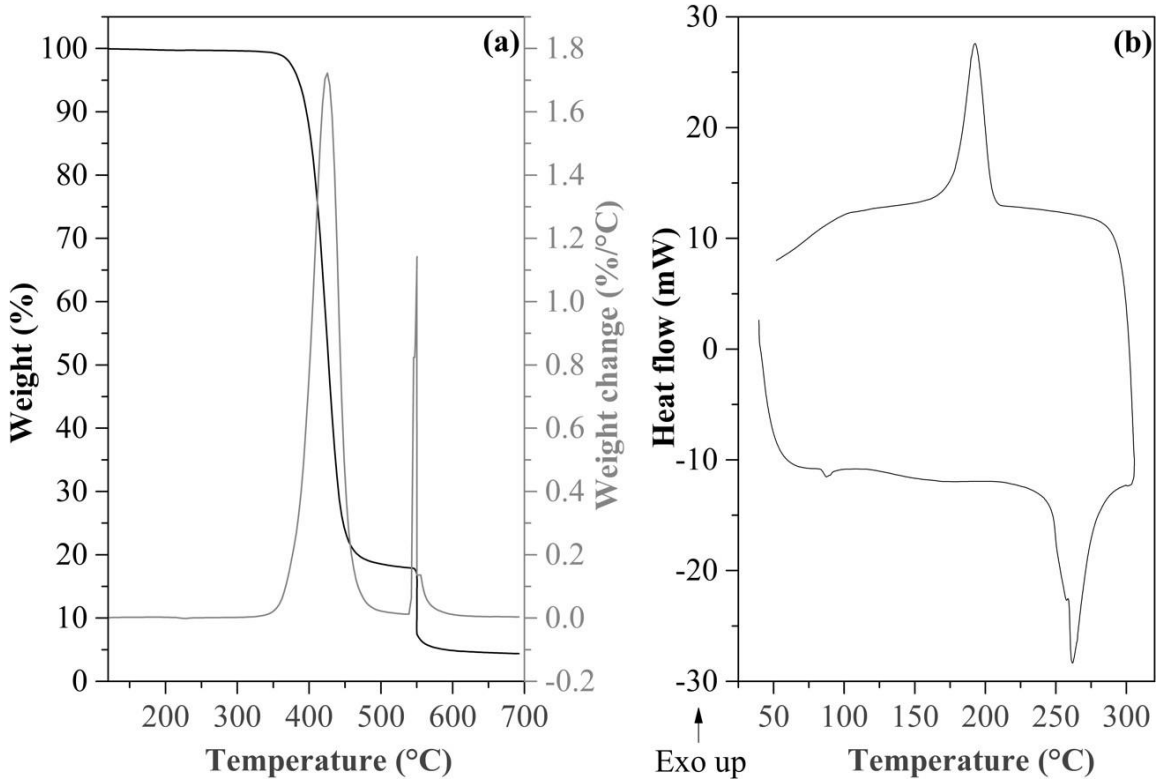

Figure 4.3. Obtained curves for PET from **(a)** TGA analysis, and **(b)** MDSC analysis

Table 4.4. T_g, T_m, T_c and T_d for the PET taken from GF/PET DREF yarns.

Temperature (°C)			
T_g	T_c	T_m	T_d
80	213	256	290

4.3.2 Consolidation by compression molding experiments

The average curves for the evolution of pressure and thickness with time obtained for the three replicates of each consolidation condition are presented in Figure 4.4. The first, second, and third columns presents the results for M1, M2, and M3, respectively. The top row corresponds to the changes in pressure with time including the standard deviations (SD). The middle row is the average thickness of the consolidation experiments measured with the laser extensometer. Note that the SD were omitted in this middle row to facilitate the observation of the behavior for each test condition. There are also two vertical lines in each of the three graphs in the m iddle row indicating the cooling start time at 4 min. and the approximate time of 18 min. when the tool was cooled below T_g. The bottom row shows a magnification of the first 4 min. including the SD to clearly differentiate the changes for each test condition before the cooling was initiated. Finally, there are horizontal dashed lines on the middle and bottom row indicating the T_{th} from **¡Error! No se encuentra el origen de la referencia.**.

The pressure versus time graphs shows that the pressure increases for 30 s to reach target pressure in all experiments according to the programmed test sequence in the UTM controller. After which, the pressure oscillates around the target values of 98, 295 and 492 kPa. The oscillations are caused by the UTM controller that constantly adjusts the actuator force to maintain the target pressure.

It is observed that there exists specific conditions of temperature and pressure at which the T_{th} for each material was obtained. Although the thickness for all the samples tends to plateau after 4 min, it was not possible to establish a steady state for thicknesses. Nevertheless, if a criterion to obtain a maximum of 5 % of distortion in thickness is considered, it is possible to establish that all the samples reached the stabilization in thickness between 8 - 10 min, when the CMT temperature was near T_c. To understand this behavior, it is relevant to mention that when PET melts, it behaves as an highly anisotropic viscous fluid that converges at different points as the GF deform [81]. Once the polymer reaches T_c, there is a reduction in the movement of the polymer network, and this is when the geometry of the laminate tends to stabilize. Below T_g the polymer has a compromised ability to retain form and structure because of its softening [75]. In the case of PET, demoulding temperature of 60 °C was defined according to what is suggested in the literature [82]. This is also a reason to ensure an intimate contact and alignment of the DREF yarns during the consolidation

process. In this case, the sample holder used prevents an abrupt transverse spreading of the yarns as the GF tend to squeeze at the bottom of the CMT when the pressure is app lied. Additionally, temperatures about 10 and 20 °C above T_m were not found to influence the SD for thickness values. This suggests that the holding time applied was enough to completely melt the PET under the range of temperatures evaluated [75].

Regarding T_{th}, it was observed that even if the difference between M2 and M3 was the twisting condition, T_{th} for both are almost equal, which can be explained by the criteria used to wind the samples before the consolidation experiments. Since the weight for all samples was constant, and M2 and M3 had equal tex and volume fractions, T_{th} was almost the same for them. Nevertheless, the conditions to obtain T_{th} for each material were different. While M2 was subjected to a pressure of 295 kPa and a temperature of 280 °C, M3 needed to be consolidated under 492 kPa and 270 °C, respectively. Similar behavior was observed for the T_{th} comparing the curves for M2P1T2 and M3P2T1. After analyzing the results obtained from the interaction between of the materials with force and temperature with a 95 % of significance level, it was possible to establish that there is no significant difference between M2 and M3. This suggests that conditions of pressure and temperature to obtain the T_{th} for these two materials are the same. Additionally, the twist may not have a significant impact on the consolidation process. It is important to note that the Taguchi design allowed the combination of different conditions of temperature and pressure, which means that every material was under subjected to different conditions. The effect of the factors needs to be established through statistical analysis. This array aimed to evaluate at least every condition of temperature and pressure for every material independently of the combination of these two factors.

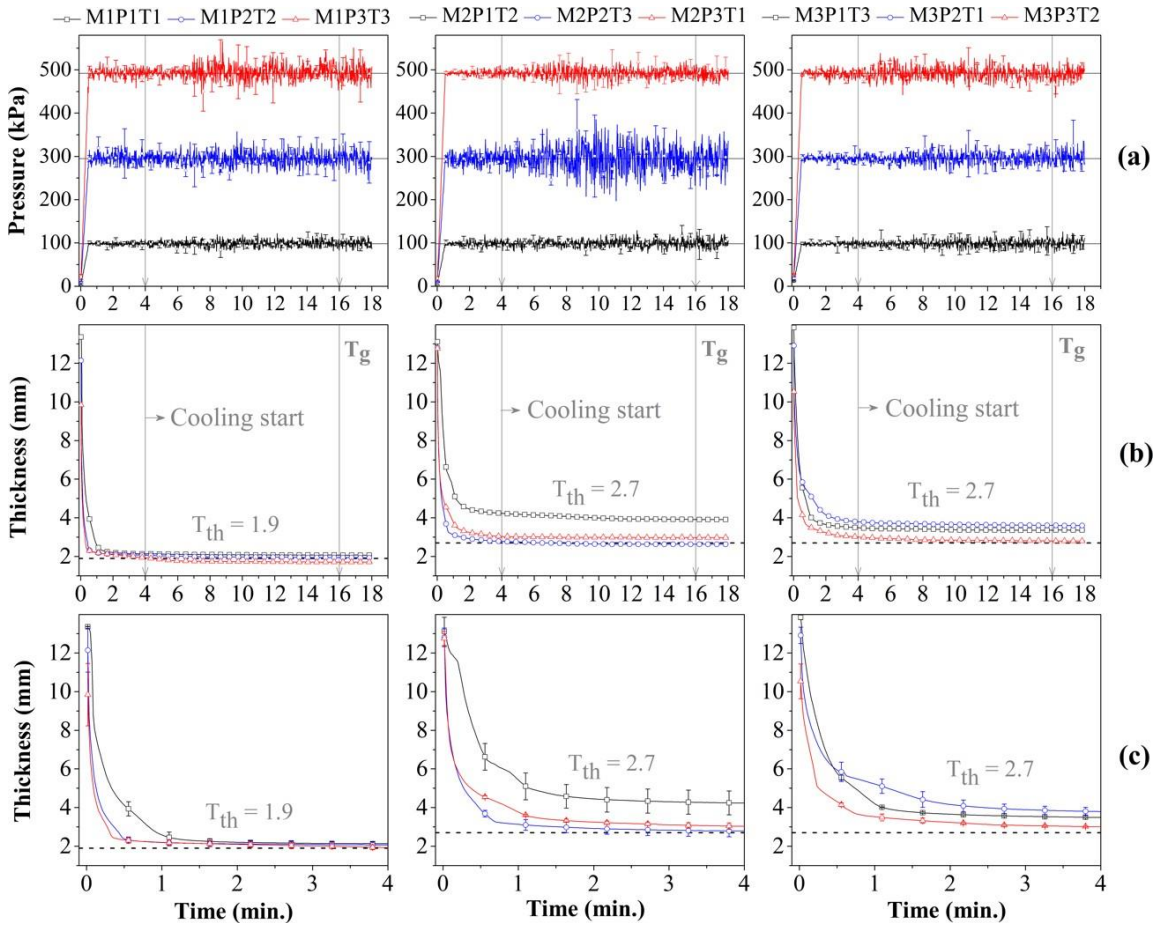

Figure 4.4. Pressure and thickness tracking during consolidation: **(a)** Average curves for Pressure (kPa) vs. Time (min.) considering SD., **(b)** Average curves for Thickness (mm) vs. Time (min.) without considering SD, and **(c)** Amplification of first 4 min. for Thickness (mm) vs. Time (min) considering SD. Dotted lines were used in (b) and (c) to facilitate the observation of the values for T_{th}

4.4 Constituent volume fractions, mechanical properties, and fracture

In Figure 4.5 shows the results for V_F, V_V and ILSS, and final thicknesses for each test condition. Figure 4.5 (a) demonstrates the relationship between the final thickness and the V_v. Greater final thicknesses are related to the samples with the highest values of V_v. This means that even if the behaviour in the consolidation curves suggested that the conditions of temperature and pressure applied were enough to reach the T_{th}, it does not necessarily convey a uniform impregnation of the

GF. Since the present study did not consider the effect of holding times, further investigations about the effect of this factor as well as the cooling rates in TPCs laminates obtained through the present methodology need to be performed to better explain these results.

Figure 4.5 (b) it is possible to observe the intimate relationship between ILSS and V_V. ILSS decreases whereas V_V increases, which is consistent with what has been reported in other studies [4][5][83]. Unidirectional TPCs made from GF reinforcing other polymer matrices such as Polyamide 6 (PA6) with similar V_F have exhibited values close to the ones obtained in the present study [84]. PA6 like PET is extensively used in the production of textiles as well as in engineering products while PET is mainly used to fabricate molded objects and textiles [85]. Even if PET presents remarkable comprehensive properties, its low impact strength has limited its use in engineering applications [86]. The obtained results may help to support the use of PET as matrix in TPCs. Also, in Figure 4.5 (b) similar values for V_F were obtained for M2 and M3 under different conditions of pressure and temperature, as well as the tendencies for V_V. It suggests that the twisting of the eight DREF tows in M3 yarns did not have a significant differencecompared to the untwisted condition in M2. This is also explained by the statistical analysis performed. It means that the twist on M3 did not influence the final properties of the consolidated laminate.

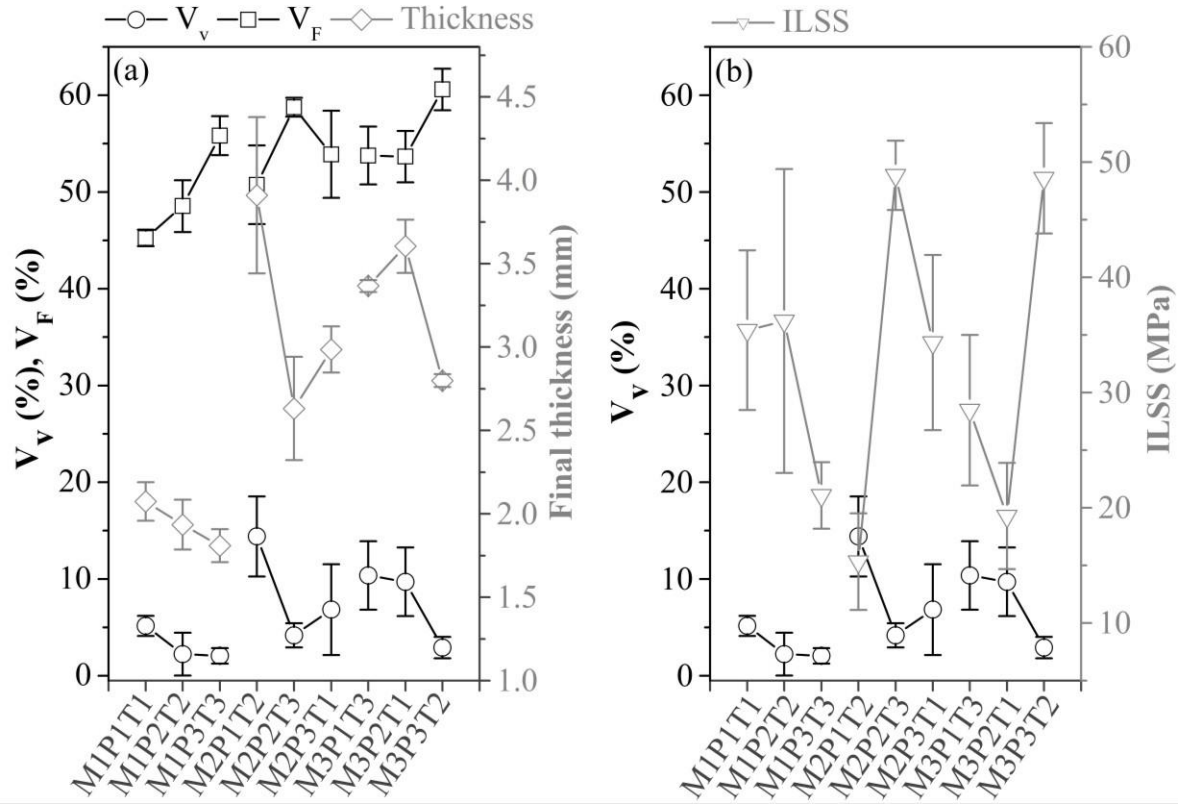

Figure 4.5. Results obtained for each test condition for: **(a)** V_F (%), V_V (%) Final thickness (mm) vs. Sample, and **(b)** V_V (%) and ILSS (MPa) vs. Sample. Lines connecting the data points were employed to better observe the tendency and relationship within the same material

Figure 4.6 shows typical micrographs at different magnifications for the materials with the lowest-M2P1T2 (Figure 4.6a) and highest-M3P3T2 (Figure 4.6b) measured ILSS. The arrows identify the GF fibers. Dark areas correspond to the voids. Light gray areas correspond to the PET polymer. Figure 6 (a) shows a large intra-tows black area displaying that the tows could not be impregnated with the PET when applying the lowest pressure of 98 kPa and the temperature of 270 °C. The dark gray areas are attributed to residual diamond solution trapped between the GF that could not be removed with the ultrasonic bath. It is also observed that GF bundles remained agglomerated keeping their oval shape. Some GFs are visible within the voids, which means that they are bound to the PET matrix at some specific points, but they are not surrounded by the polymer. The combination of the polishing actions and voids also damaged the GF, what is clearer in Figure 4.6 (b). Regarding the zones where the voids are present, it is observed micro and macro voids. Since the geometry of the CMT did not have any insert, ribs, or cores, it is possible to attribute the

presence of macro-voids to the permeability of the DREF yarns, and the possible differences in the flow patterns of the PET during its melting [51]. Micro-voids are created when the high viscosity of the polymer prevent its flow between the fibers [53], where the time to allow full impregnation is too short, or the pressure driving the flow is too low. Although this study does not cover the rheological properties of the PET, it is possible to establish that there exist conditions of pressure and temperature for which these defects are not predominant in the consolidated laminate. This statement is also supported by the micrograph shown in Figure 4.6 (c), where the microstructure of M3P3T2 shows the GF well distributed, the yarn boundaries are undistinguishable, and voids are virtually inexistent. Figure 4.6 (d) shows that the GF did not present any damage from surface preparation. That is attributed to the fact the GF are surrounded by the PET matrix. The main differences between M2P1T2 and M3P3T2 consolidation experiments are the twist applied to the yarns in M3, and the consolidation pressure rising from 98 kPa in M2P1T2 to 492 kPa in M3P3T2. Since the same temperature and consolidation time were applied for both cases, it is assumed that the viscosity of PET did not influence the impregnation. Therefore, it is possible to conclude that a 5 times higher pressure (P1 to P3) was the main driver for better impregnation.

It is also pertinent to mention that the voids observed in M2P1T2 were only formed in the areas where GF were present, it means that there were no voids formed within the matrix. This fact may indicate that if in case was air trapped within the matrix during the consolidation traveled to the areas where unimpregnated GF were located [51]. Besides this, Mondadori et *al*. reported the importance of the adhesion between the GF and PET [87]. They evaluated GF/PET composites using two different surface functionalized GF with amine and epoxy. They found both treatments enhanced the obtention of GF/PET composites with remarkable flexural strength and impact resistance. In the case of the present study, the nature of the sizing applied to the GF by the manufacturer is unknown [88]. According to manufacturer, the sizing applied is compatible with some thermoplastics such as PEI, PA, and PEEK. Nevertheless is uncertain if the differences in the nature of the PET respect to the compatible polymers could have also an affect the impregnation of the GF [87].

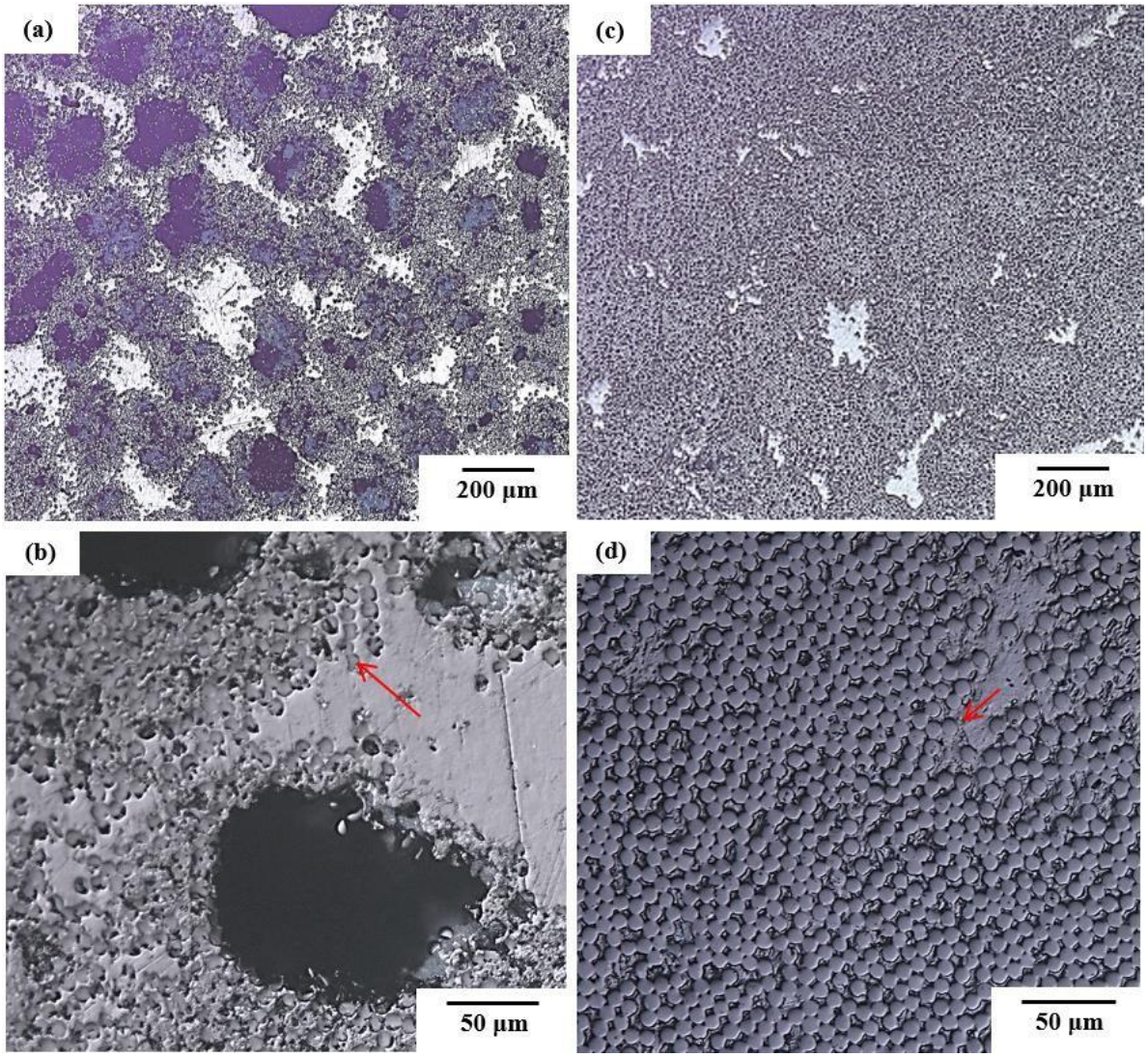

Figure 4.6. Micrographs of the polished cross section surfaces obtained from the consolidated laminates of: (a) M2P1T2 at 100x, (b) M2P1T2 at 500x, (c) M3P3T2 at 100x, and (c) M3P3T2 at 500x. Arrows were used to identify some GF

SEM images of the fracture surface from interlaminar shear strength evaluation for M2P1T2 and M3P3T2 are presented in Figure 4.7. Figure 4.7 (a-c) shows the images for M2P1T2 at different magnifications. It is possible to clearly identify the areas where there are unimpregnated GF, and the crack surrounded by the dry GF. For M3P3T2 the scenario is different, Figure 4.7 (d-f) shows how the GF were impregnated by the PET polymer, where in the two main cracks the constituents behave as a composite. The fracture surfaces for both samples are consistent with Figure 4.6.

Higher magnifications images were obtained for areas near the center of each coupon, where the load was applied. It is relevant to mention that since the rectangular coupons were obtained via cutting operations, the unimpregnated GF were directly affected by the cutter, and that is why GFs are visible out from the PET matrix. In the case of M3P3T2, the consolidated laminate behaved as a unit, i.e., the GF are bonded to the PET matrix, and they were protected by the latter during the cutting. It was also observed that for both samples, the interlaminar shear surfaces e xhibited delamination of the PET matrix. It implies that the DREF yarns wound formed layers of material during consolidation process. Since the winding procedure applied in this study assured the straightness of the DREF yarns and the presence of waviness and uneven GF, the results obtained for ILSS as well as the fracture surfaces related to them correspond to typical shear stress created between the formed layers [89].

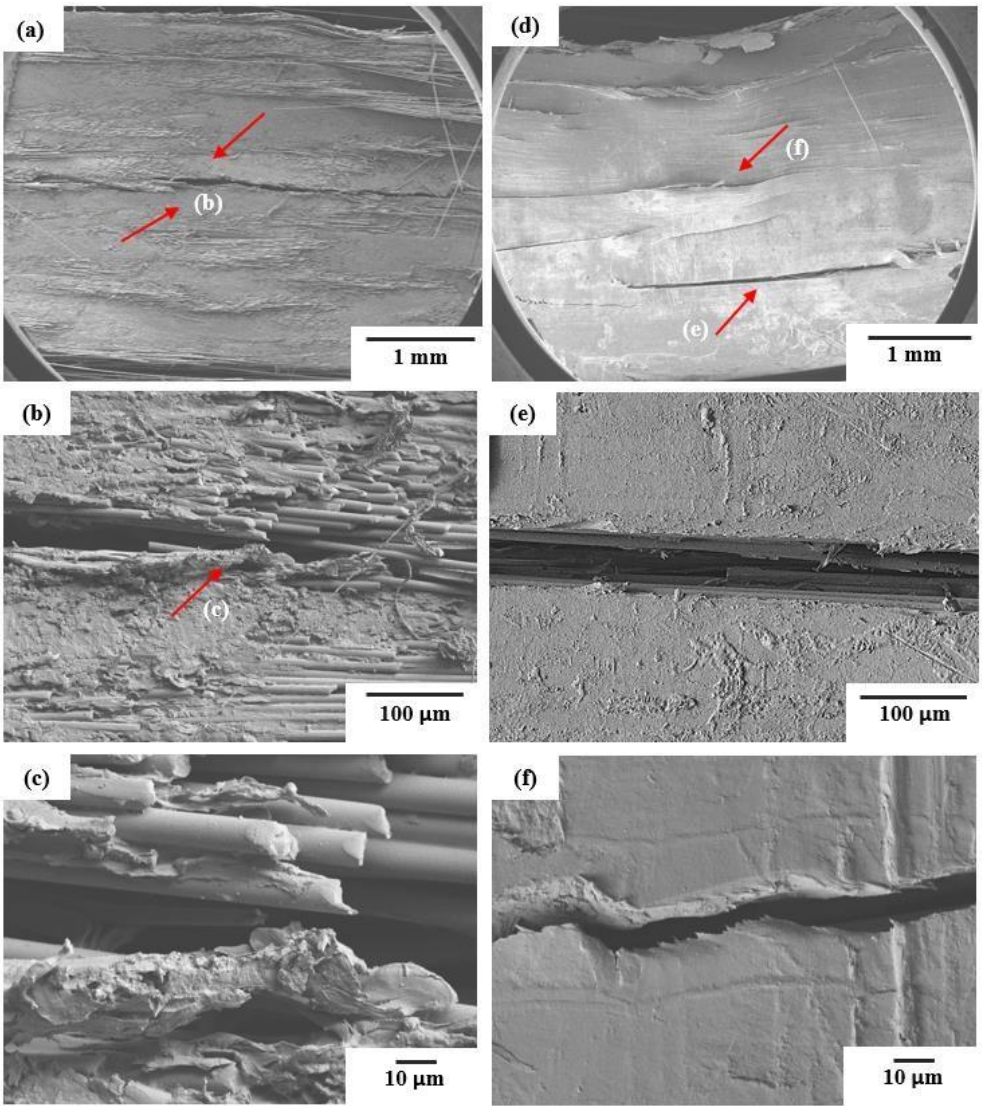

Figure 4.7. SEM images of the fracture surfaces from interlaminar shear strength: **(a)** M2P1T2, **(b)** Amplification of the surface presented in (a), **(c)** Amplification of the surface presented in (b), **(d)** M3P3T2, **(e)** and **(f)** Amplifications of the two fracture surfaces presented in (d)

4.5 Taguchi analysis method to obtain the laminates with the best performance

The criteria to select the final characteristics to determine the consolidated laminate with the best performance are shown in Table 4.5. In the case of T_{th}, the consolidation conditions are reported for each material. According to the microstructural and mechanical characterization, voids in this study are considered defects, so, the criteria was based on obtaining a consolidated laminate with the lowest V_v. For ILSS, the highest values were looked for. The lowest value for V_v was achieved

with M1; it can be explained by the lower Tex of M1 compared to M2 and M3. It means that the molten PET needed to travel shorter distances to cover the GF. This is also supported by Figure 1 where the differences in the DREF yarns diameters were observed. These results are useful to determine possible conditions to obtain the consolidated sample with the best performance according to the pre-established criteria.

Table 4.5. Selection of consolidation conditions to obtain the consolidated laminate with the best performance.

Property/Characteristic	Criteria	Consolidation conditions
V_V	Smaller the better	Pressure of 492 kPa (P3), and a temperature of 280 °C (T3) using M1
ILSS	Higher the better	Pressure of 492 kPa (P3), and a temperature of 280 °C (T3) using either M2 or M3
T_{th}	Nominal the better	M1: 295 kPa (P2) and 270 °C (T2) M2: 295 kPa (P2) and 280 °C (T3) M3: 492 kPa (P3) and 270 °C (T2)

4.6 Conclusions

The consolidation by compression molding of TPCs made from GF/PET DREF yarns have been investigated with respect to the effects of processing parameters on the ILSS and the void fractions. DREF architecture is shown to benefit the polymer flow through the reinforcing fiber, and more uniform consolidation of the yarns. They have the advantage to protect the reinforcement during handling operations, which is limited with common hybrid yarns like commingled where the polymer filaments are intermixed. The methodology applied in this study helped to keep the fibers aligned during consolidation and allowed the fabrication of laminates that represent the final mechanical properties of unidirectional TPCs. According to the statistical analysis performed, it was possible to demonstrate that the applied twist on the GF/PET DREF yarns did not have a

significant effect on the final properties of the consolidated laminates. The application of pressures as high as 492 kPa with a temperature 20 °C greater than the melting temperature of the PET reduced the void volume fractions to below 5%. Additionally, the conditions for the obtention of the nominal thickness for each material were determined. The advantage of tracking thicknesses changes with a UTM equipped with a laser extensometer is that there is no physical interference in the consolidation process caused by the installation of tools that require direct contact with the sample. This method can be used in future investigations to provide additional control over the consolidation of thermoplastic composites. Further studies in the consolidation behavior of this DREF precursor can provide additional tools for the understanding, optimization, and modeling of future manufacturing processes.

It was found that GF reinforcing TPCs with other matrices such as PA6 presented similar values for the evaluated mechanical properties. Since the use of PET is widely known and standardized in textile industry, this fact may open the doors to use DREF yarns as a precursor of unidirectional TPCs with PET as the matrix. Further studies of different cooling rates will help to understand the behavior of the PET during consolidation to analyze how the viscoelastic nature of the PET can affect the impregnation in TPCs made from DREF yarns. Finally, additional studies about the effect of the sizing applied to the GF may be relevant to determine its significance in the impregnation of GF during consolidation through compression molding.

CHAPTER 5 GENERAL DISCUSSION

The presented work aims to increase the interest in using new precursors from hybrid yarns to produce TPCs. DREF process may present advantages such as the high production rates as well as the possibility of tailoring the core-to-sheath ratio with flexibility. The use of PET as thermoplastic matrix for TPCs from DREF yarns also represents an innovation regarding other commodity matrices used in composites industry such as polyamides and polypropylene, with the advantage of having PET as one of the most used polymers in textiles production.

The interest of researchers in tracking different variables during consolidation of TPCs has leaded the development of different systems and methodologies with this task. The design of a system that could be adapted to a universal testing machine to track the evolution of the consolidation process by using a temperature controller and a laser extensometer, provided accurate measurements in distances, which allowed to perform an intimate analysis of the thicknesses during the application of pressure. This can be used in future works along with modelling to predict the final thickness of samples made of this DREF precursor, what can provide additional tools for the control of the final product dimensions and microstructure.

The development of a winding method to standardize the unidirectional alignment of the yarns is an innovative way of reducing and prepare samples that accurately represent the distribution of unidirectional composites. This method can be also use with other precursors such as commingled to compare its behaviour with DREF yarns.

On the other hand, PET is around 30 percent cheaper in comparison to other common thermoplastic fibers such as polyamide 6, which represents a decrease in the costs of production of hybrid yarns with this thermoplastic matrix.

CHAPTER 6 CONCLUSION

6.1 Synthesis of the work

The research presented is an evaluation to study the consolidation behaviour of unidirectional thermoplastic composites made from hybrid DREF yarns. The principal objective of th is thesis was to evaluate the effect of temperature and pressure during consolidation of unidirectional from different DREF yarns by controlling the applied pressure, temperature, and thickness evolution. The accomplishment of this objective was obtainedby the achievement of sub-objectives that were presented at the beginning of this thesis.

The development of a methodology to prepare preforms for the consolidation of unidirectional thermoplastic composites by winding method demonstrated the advantage of keeping the alignment of the yarns, and a constant final tension in all the wound samples. The thermal characterization of the PET provided the temperature range at which the DREF yarns could be consolidated by compression molding without being highly affected by degradation phenomena. DREF yarns with different Tex, volume fractions, and twisting conditions were evaluated to determine their behaviour during consolidation by compression molding at different pressures and temperatures. The work submitted to the journal Composites Part A shows the evolution in thickness and pressure during the consolidation of DREF yarns. The final volume fractions for void and glass, and the short-beam strength were evaluated for the obtained laminates. The conditions for the obtention of the nominal thickness for each of the DREF yarns evaluated was successfully achieved. A temperature of 280 °C, and a pressure of 492 kPa were the conditions defined as the most adequate to obtain unidirectional laminates with a void volume fraction below 5 %, with a short-beam strength of about 62 MPa, using a 60/40 volume fraction of GF/PET DREF yarns previously twisted or untwisted.

Finally, the results presented demonstrated the feasibility of using hybrid yarns like DREF to produce unidirectional thermoplastic composites from a commodity polymer like PET, and it also opens the doors to cover other aspects to understand the impregnation behaviour in this type of hybrid yarns.

6.2 Limitations of this study and future work

The methodology designed and followed in this study allowed the evaluation of the consolidation behaviour of hybrid yarns like DREF to obtain unidirectional thermoplastic composites. However, the cooling rates for the demolding were not studied. The criteria to demold the consolidated laminates was at a temperature of 60 °C (below T_g) in the compression molding tooling. Since PET is a semicrystalline thermoplastic, the effect of cooling rates may have an impact on the consolidation behaviour. Additionally, the rheology of PET at the applied temperatures during consolidation should be assessed to understand the role of the polymer viscosity in the consolidation, and in the impregnation of the reinforcement fibers.

REFERENCES

[1] T. Ngo, *Composites and Nanocomposites Materials: From Knowledge to Industrial Applications*. London, United Kingdom, 2020. doi: 10.5772/intechopen.80186.

[2] P. Sivasubramanian, K. Mayandi, V. Arumugaprabu, N. Rajini, and S. Rajesh, *Polymer - Based Composites: Design, Manufacturing, and Applications*, no. July. CRC Press, 2021. doi: 10.1201/9781003126300-1.

[3] A. Suresh G. and E. M. Sozer, "Advanced Thermoplastic Composite Manufacturing Processes," in *Process Modeling in Composites Manufacturing*, A. Suresh G. and M. S. E., Eds. CRC Press, 2003, p. 48. [Online]. Available: https://www.taylorfrancis.com/chapters/mono/10.1201/9780203910061-8/advanced-thermoplastic-composite-manufacturing-processes-suresh-advani-murat-sozer?context=ubx&refId=d02d250c-40e4-43db-8227-47041cab72ff

[4] H. R. Mankodi, "Developments in hybrid yarns," *Spec. Yarn Fabr. Struct.*, pp. 21–55, 2011, doi: 10.1533/9780857093936.21.

[5] J. Bijwe, M. Sharma, W. Hufenbach, K. Kunze, and A. Langkamp, *Surfaceengineering with micro- and nanosized solid lubricants for enhanced performance of polymer composites and bearings*, Second Edi. Elsevier, 2013. doi: 10.1016/B978-0-444-59455-6.00020-9.

[6] J. J. Rocher *et al.*, "Experimental characterization and modeling of GF / PP commingled yarns tensile behavior To cite this version : HAL Id : hal-01071017," *J. Compos. Mater.*, vol. 49, no. 21, pp. 2609–2624, 2015, doi: 10.1177/0021998314551035.Abstract.

[7] D. E. Fehrer, "DREF - 3 FT System." Fehrer AG, Linz, Austria, 1995.

[8] H. V. Shaw, "Friction spinning," *Text. Prog.*, no. May 2013, pp. 37–41, 1988, doi: 10.1080/00405160308688958.

[9] B. J. McCarthy, "1 - An overview of the technical texitles sector," in *Handbook of Technical Textiles*, A. R. Horrocks and S. C. Anand, Eds. Woodhead Publishing, 2016, pp. 1–20. doi: https://doi.org/10.1016/B978-1-78242-458-1.00001-7.

[10] S. Kumartasli and O. Avinc, "Recycled Thermoplastics: Textile Fiber Production, Scientific and Recent Commercial Developments," in *Recent Developments in Plastic Recycling*, J.

Parameswaranpillai, S. Mavinkere Rangappa, G. Rajkumar, and S. A., Siengchin, Eds. Singapore: Springer, Singapore, 2021, pp. 169–192. doi: https://doi.org/10.1007/978-981-16-3627-1_8.

[11] C. A. Lawrence, *SPUN YARN TECHNOLOGY*. CRC Press, 2003.

[12] J. N. F. D. Motaj. P. L. GIL, "Pultrusion head to produce long fibre reinforced thermoplastic matrix profiles," WO2002006037A1, 2000

[13] T. Gries, M. Raina, T. Quadflieg, and O. Stolyarov, "1 - Manufacturing of textiles for civil engineering applications," in *Textile Fibre Composites in Civil Engineering* , T. Triantafillou, Ed. Woodhead Publishing, 2016, pp. 3–24. doi: https://doi.org/10.1016/B978-1-78242-446-8.00002-1.

[14] A. R. Horrocks and S. C. Anand, *Handbook of technical textiles. Volume 1, Technical textile processes*, vol. 1, no. 169. 2017.

[15] B.-D. Choi, O. Diestel, and P. Offermann, "Commingled CF/PEEK Hybrid Yarns for Use in Textile Reinforced High Performance Rotors," *12th Int. Conf. Compos. Mater.*, pp. 796–806, 1999, [Online]. Available: http://www.iccm-central.org/Proceedings/ICCM12proceedings/site/papers/pap528.pdf

[16] G. M. Abbott, "Wrapped-yarn reinforced composites: Part I-yarn properties," *Compos. Sci. Technol.*, vol. 24, no. 2, pp. 147–158, 1985, doi: 10.1016/0266-3538(85)90056-9.

[17] A. Mirdehghan, H. Nosraty, M. M. Shokrieh, and M. Akhbari, "The structural and tensile properties of glass/polyester co-wrapped hybrid yarns," *J. Ind. Text.*, vol. 47, no. 8, pp. 1979–1997, 2018, doi: 10.1177/1528083717716166.

[18] B. Baghaei, M. Skrifvars, and L. Berglin, "Manufacture and characterisation of thermoplastic composites made from PLA/hemp co-wrapped hybrid yarn prepregs," *Compos. Part A Appl. Sci. Manuf.*, vol. 50, pp. 93–101, 2013, doi: 10.1016/j.compositesa.2013.03.012.

[19] Vogelsang and et al, "US005464684A," 5,464,684, 1995

[20] I. VERPOEST, "Composite Preforming Techniques," in *Comprehensive Composite Materials*, Elsevier Inc., 2000, pp. 623–669. doi: 10.1016/b0-08-042993-9/00168-6.

[21] Y. E. Elmogahzy, “Yarns,” in *Engineering Textiles*, 2020, pp. 223–248. doi: 10.1016/b978-0-08-102488-1.00009-5.

[22] M. Bar, A. Das, and R. Alagirusamy, “Effect of interface on composites made from DREF spun hybrid yarn with low twisted core flax yarn,” *Compos. Part A Appl. Sci. Manuf.*, vol. 107, pp. 260–270, 2018, doi: 10.1016/j.compositesa.2018.01.003.

[23] M. M. B. Hasan, S. Nitsche, A. Abdkader, and C. Cherif, “Carbon fibre reinforced thermoplastic composites developed from innovative hybrid yarn structures consisting of staple carbon fibres and polyamide 6 fibres,” *Compos. Sci. Technol.*, vol. 167, pp. 379–387, 2018, doi: 10.1016/j.compscitech.2018.08.030.

[24] S. Roychowdhury and S. G. Advani, “An experimental investigation of consolidation in thermoplastic filament winding,” *Compos. Manuf.*, vol. 2, no. 2, pp. 97–104, 1991, doi: 10.1016/0956-7143(91)90186-K.

[25] L. Feuillerat, O. De Almeida, J. C. Fontanier, and F. Schmidt, “Effect of poly(ether ether ketone) degradation on commingled fabrics consolidation,” *Compos. Part A Appl. Sci. Manuf.*, vol. 149, no. February, p. 106482, 2021, doi: 10.1016/j.compositesa.2021.106482.

[26] M. D. Wakeman and J. A. E. Månson, “Composites manufacturing - thermoplastics,” in *Design and Manufacture of Textile Composites*, 2005, pp. 197–241. doi: 10.1533/9781845690823.197.

[27] M. Biron, “Thermoplastic Composites,” in *Thermoplastics and Thermoplastic Composites*, M. Biron, Ed. William Andrew Publishing, 2018, pp. 821 –882. doi: https://doi.org/10.1016/B978-0-08-102501-7.00006-0.

[28] S. Erden and K. Ho, “Fiber reinforced composites,” in *Fiber Technology for Fiber-Reinforced Composites*, M. Ö. Seydibeyoğlu, A. K. Mohanty, and M. Misra, Eds. Woodhead Publishing, 2017, pp. 51–79. doi: 10.1016/B978-0-08-101871-2.00003-5.

[29] M. Biron, *Industrial Application of Renewable Plastics*. Elsevier, 2016.

[30] J. P. Srivastava and P. Kumar, “Introduction to Glass Fiber-Based Composites and Structures,” *Natural and Synthetic Fiber Reinforced Composites*. pp. 1–16, 2022. doi: 10.1002/9783527832996.ch1.

[31] K. Joseph, K. Oksman, G. George, R. Wilson, and S. Appukuttan, Eds., “Fiber reinforced composites for aerospace and sports applications,” in *Fiber Reinforced Composites*, Woodhead Publishing, 2021, pp. 821–859. doi: https://doi.org/10.1016/B978-0-12-821090-1.00023-5.

[32] B. Sun and J. Yu, “High-Perfomance Composites and Their Applications,” in *Porous Lightweight composites reinforced with fibrous structures*, Y. Yang, J. Yu, H. Xu, and B. Sun, Eds. Germany: Springer, Berlin, Heidelberg, 2017, pp. 341 –368. doi: https://doi.org/10.1007/978-3-662-53804-3_13.

[33] K. Yassin and M. Hojjati, “Processing of thermoplastic matrix composites through automated fiber placement and tape laying methods: A review,” *J. Thermoplast. Compos. Mater.*, vol. 31, no. 12, pp. 1676–1725, 2018, doi: 10.1177/0892705717738305.

[34] D. Y, Ng. T-L, L. D, L. S, and L. A., “Thick thermoplastic composite laminate consolidation: Experimental observations and numerical approaches,” *J. Compos. Mater.*, vol. 56, no. 4, pp. 2169–2188, 2022, doi: doi:10.1177/00219983221090578.

[35] R. Alagirusamy, “Hybrid yarns for thermoplastic composites,” in *Technical Textile Yarns*, 2010, pp. 387–428. doi: 10.1533/9781845699475.2.387.

[36] J. W. Seo and W. il Lee, “A Model of the Resin Impregnation in Thermoplastic Composites,” *J. Compos. Mater.*, vol. 25, no. 9, pp. 1127–1142, 1991, doi: 10.1177/002199839102500903.

[37] H. Darcy, *Les fontaines publiques de la ville de Dijon: Exposition et application des principes à suivre et des formules à employer dans les questions de distribution d’eau : Ouvrage terminé par un appendice relatif aux fournitures d’eau de plusieurs villes, au fil*. V. Dalmont, 1856.

[38] F. J. Valdes-Parada, J. A. Ochoa-Tapia, and J. Alvarez-Ramirez, “Validity of the permeability Carman-Kozeny equation: A volume averaging approach,” *Phys. A Stat. Mech. its Appl.*, vol. 388, no. 6, pp. 789–798, 2009, doi: 10.1016/j.physa.2008.11.024.

[39] A. Miller and A. G. Gibson, “Impregnation technology for thermoplastic matrix composites,” *Polym. Polym. Compos.*, vol. 4, no. 7, pp. 459–481, 1996.

[40] M. Rahrah, L. A. Lopez-Peña, F. Vermolen, and B. Meulenbroek, “Network-inspired versus

Kozeny–Carman based permeability-porosity relations applied to Biot's poroelasticity model," *J. Math. Ind.*, vol. 10, no. 1, 2020, doi: 10.1186/s13362-020-00087-z.

[41] T. G. Gutowski, Z. Cai, S. Bauer, D. Boucher, J. Kingery, and S. Wineman, "Consolidation Experiments for Laminate Composites," *J. Compos. Mater.*, vol. 21, no. 7, pp. 650–669, 1987, doi: 10.1177/002199838702100705.

[42] V. Michaud and J. A. E. Månson, "Impregnation of compressible fiber mats with a thermoplastic resin. Part I: Theory," *J. Compos. Mater.*, vol. 35, no. 13, pp. 1150–1173, 2001, doi: 10.1106/8108-1VMC-B4FG-FXPU.

[43] V. Michaud, R. Törnqvist, and J.-A. E. Månson, "Impregnation of Compressible Fiber Mats with a Thermoplastic Resin. Part II: Experiments," *J. Compos. Mater.*, vol. 35, no. 13, pp. 1174–1200, 2001, doi: 10.1177/002199801772662280.

[44] A. M. Murtagh, A. J. Mulholland, M. R. Monaghan, and P. J. Mallon, "Aspects in Sheet-Forming Characterisation of Advanced Composites," *Key Eng. Mater.*, vol. 72–74, pp. 263–278, 1992, doi: 10.4028/www.scientific.net/kem.72-74.263.

[45] A. Hautefeuille, S. Comas-Cardona, and C. Binetruy, "Mechanical signature and full-field measurement of flow-induced large in-plane deformation of fibrous reinforcements in composite processing," *Compos. Part A Appl. Sci. Manuf.*, vol. 118, no. December 2018, pp. 213–222, 2019, doi: 10.1016/j.compositesa.2018.12.030.

[46] A. Hautefeuille, S. Comas-Cardona, and C. Binetruy, "Consolidation and compression of deformable impregnated fibrous reinforcements: Experimental study and modeling of flow-induced deformations," *Compos. Part A Appl. Sci. Manuf.*, vol. 131, no. February, p. 105768, 2020, doi: 10.1016/j.compositesa.2020.105768.

[47] A. E. Pasto, D. N. Braski, T. R. Watkins, W. D. Porter, E. Lara-Curzio, and S. B. McSpadden, "Characterization techniques for composites and other advanced materials," *Compos. Part B Eng.*, vol. 30, no. 7, pp. 631–646, 1999, doi: 10.1016/S1359-8368(99)00040-2.

[48] S. R. Bym, G. Zografi, and X. Chen, "Differential Scanning Calorimetry and Thermogravimetric Analysis," in *Solid-State Properties of Pharmaceutical Materials*, 1st ed., S. R. Byrn, G. Zografi, and X. Chen, Eds. New York: John Wiley & Sons, Inc, 2017.

doi: 10.1002/9781119264408.ch10.

[49] K. Friedrich, *Fractographic Analysis of Polymer Composites*, vol. 6, no. C. Elsevier Science Publishers B.V., 1989. doi: 10.1016/B978-0-444-87286-9.50015-2.

[50] J. Hajsman, S. Jenicek, L. Kucerova, and D. Rieger, "Microstructure and Properties of Polymer Composites," *Manuf. Technol.*, vol. 19, no. 6, pp. 941–946, 2019, doi: 10.21062/ujep/400.2019/a/1213-2489/mt/19/6/941.

[51] M. Mehdikhani, L. Gorbatikh, I. Verpoest, and S. V. Lomov, "Voids in fiber-reinforced polymer composites: A review on their formation, characteristics, and effects on mechanical performance," *J. Compos. Mater.*, vol. 53, no. 12, pp. 1579–1669, 2019, doi: 10.1177/0021998318772152.

[52] Q. Song *et al.*, "Research on Void Dynamics during In Situ Consolidation of CF/High-Performance Thermoplastic Composite," *Polymers (Basel).*, vol. 14, no. 7, 2022, doi: 10.3390/polym14071401.

[53] A. Hyde, J. He, X. Cui, J. Lua, and L. Liu, "Effects of microvoids on strength of unidirectional fiber-reinforced composite materials," *Compos. Part B Eng.*, vol. 187, no. January, p. 107844, 2020, doi: 10.1016/j.compositesb.2020.107844.

[54] J. C. Russ and F. Brent Neal, *The Image Processing*, 7th ed. Boca Raton, 2016. doi: 10.1201/b18983.

[55] C. R. Brooks and B. L. McGill, "The application of scanning electron microscopy to fractography," *Mater. Charact.*, vol. 33, no. 3, pp. 195–243, 1994, doi: https://doi.org/10.1016/1044-5803(94)90045-0.

[56] R. W. Cahn, "Quantitative image analysis of microstructures," *Adv. Mater.*, vol. 2, no. 2, pp. 111–112, 1990, doi: 10.1002/adma.19900020216.

[57] J. M. Machado, J. M. R. S. Tavares, P. P. Camanho, and N. Correia, "Automatic void content assessment of composite laminates using a machine-learning approach," *Compos. Struct.*, vol. 288, no. April 2021, 2022, doi: 10.1016/j.compstruct.2022.115383.

[58] K. J. Bowles and S. Frimpong, "Relationship between voids and interlamina r shear strength of polymer matrix composites," *Int. SAMPE Symp. Exhib.*, vol. 36, no. pt 2, pp. 1631–1648,

1991.

[59] I. Tretiak, L. F. Kawashita, and S. R. Hallett, “Predicting short beam shear strength reduction in carbon/epoxy laminates containing voids,” *Compos. Struct.*, vol. 290, no. November 2021, p. 115472, 2022, doi: 10.1016/j.compstruct.2022.115472.

[60] Y. Sun, Y. Lu, and X. Guo, “The effects of sample preparation on the interlaminar shear strength test values of unidirectional carbon fiber-reinforced epoxy composites,” *Polym. Polym. Compos.*, vol. 27, no. 4, pp. 228–234, 2019, doi: 10.1177/0967391118824817.

[61] T. G. Gutowski, T. Morigaki, and Z. Cai, “The Consolidation of Laminate Composites,” *J. Compos. Mater.*, vol. 21, no. 2, pp. 172–188, 1987, doi: 10.1177/002199838702100207.

[62] V. Michaud, “14 - Permeability properties of reinforcements in composites,” in *Composite Reinforcements for Optimum Performance*, 2011, pp. 431–457. doi: 10.1533/9780857093714.3.431.

[63] M. Ono, M. Yamane, S. Tanoue, H. Uematsu, and Y. Yamashita, “Mechanical properties of thermoplastic composites made of commingled carbon fiber/nylon fiber,” *Polymers (Basel).*, vol. 13, no. 19, pp. 3–9, 2021, doi: 10.3390/polym13193206.

[64] L. Li, S. Wang, and J. Yu, “Mechanical properties of commingled yarn composites,” *Indian J. Fibre Text. Res.*, vol. 27, no. 3, pp. 287–289, 2002.

[65] D. K. Rajak, D. D. Pagar, P. L. Menezes, and E. Linul, “Fiber-reinforced polymer composites: Manufacturing, properties, and applications,” *Polymers (Basel).*, vol. 11, no. 10, 2019, doi: 10.3390/polym11101667.

[66] E. Madeer, K. Skop-Cardarella, W. Zah, and G. Wagener, “Thermoplastic Composites,” in *Thermoplastics and Thermoplastic Composites*, vol. 32, no. 1, 1998, pp. 821–882. doi: 10.1016/B978-0-08-102501-7.00006-0.

[67] V. K. Maes, A. Radhakrishnan, J. Hartley, S. Sykes, and J. Kratz, “Tracking consolidation of out-of-autoclave prepreg corners using pressure sensors,” *Compos. Part A Appl. Sci. Manuf.*, vol. 163, no. May, p. 107172, 2022, doi: 10.1016/j.compositesa.2022.107172.

[68] R. Kleicke, A. Mountasir, C. Cherif, G. Hoffmann, and C. Franz, “Thermoplastic fiber-reinforced composites based on noncrimped and multilayered weaves,” *J. Thermoplast.*

Compos. Mater., vol. 27, no. 10, pp. 1370–1386, 2014, doi: 10.1177/0892705712473622.

[69] and İ. H. Ç. M. Kurban, O. Babaarslan, "Hybrid Yarn Composites for Construction," in *Textiles for Advanced Applications*, B. Kumar and S. Thakur, Eds. London, United Kingdom: IntechOpen, 2017. [Online]. Available: https://www.intechopen.com/chapters/55992 doi: 10.5772/intechopen.69034

[70] V. . Zhokhovskii, "Doubling process," *The Great Sovietic Encyclopedia*. pp. 1970–1979, 2010. [Online]. Available: https://encyclopedia2.thefreedictionary.com/Doubling

[71] T. E. of E. Britannica, "Twisting," *Encyclopedia Britannica*, 1998. https://www.britannica.com/technology/twisting

[72] H. Xiong, N. Hamila, and P. Boisse, "Consolidation modeling during thermoforming of thermoplastic composite prepregs," *Materials (Basel).*, vol. 12, no. 18, pp. 10–18, 2019, doi: 10.3390/ma12182853.

[73] G. L. Batch, S. Cumiskey, and C. W. Macosko, "Compaction of fiber reinforcements," *Polym. Compos.*, vol. 23, no. 3, pp. 307–318, 2002, doi: 10.1002/pc.10433.

[74] A. Koptelov, J. P. H. Belnoue, I. Georgilas, S. R. Hallett, and D. S. Ivanov, "Revising testing of composite precursors – A new framework for data capture in complex multi-material systems," *Compos. Part A Appl. Sci. Manuf.*, vol. 152, no. October 2021, p. 106697, 2022, doi: 10.1016/j.compositesa.2021.106697.

[75] M. A. Valverde, J. P. H. Belnoue, R. Kupfer, L. F. Kawashita, M. Gude, and S. R. Hallett, "Compaction behaviour of continuous fibre-reinforced thermoplastic composites under rapid processing conditions," *Compos. Part A Appl. Sci. Manuf.*, vol. 149, no. June, p. 106549, 2021, doi: 10.1016/j.compositesa.2021.106549.

[76] A. Hautefeuille, S. Comas-Cardona, and C. Binetruy, "Consolidation and compression of deformable impregnated fibrous reinforcements: Experimental study and modeling of flow-induced deformations," *Compos. Part A Appl. Sci. Manuf.*, vol. 131, no. July 2019, p. 105768, 2020, doi: 10.1016/j.compositesa.2020.105768.

[77] S. A. Fraley *et al.*, "14 . 1 : DESIGN OF EXPERIMENTS VIA TAGUCHI METHODS - ORTHOGONAL," pp. 1–10.

[78] B. Demirel, A. Yaraş, and H. Elçiçek, "Crystallization Behavior of PET Materials," *BAÜ Fen Bil. Enst. Derg. Cilt*, vol. 13, no. 1, pp. 26–35, 2011.

[79] T. Instruments, "PET Analysis by Rapid Heat-Cool DSC." pp. 1–3, 2000. [Online]. Available: https://www.tainstruments.com/pdf/literature/TA352 PET Analysis by Rapid Heat-Cool DSC.pdf

[80] A. S. C. Rego, A. de Santana, A. V. Grillo, and B. F. Santos, "Thermogravimetric study of raw and recycled polyethylene using genetic algorithm for kinetic parameters estimation," *Chem. Eng. Trans.*, vol. 74, no. May 2018, pp. 145–150, 2019, doi: 10.3303/CET1974025.

[81] T. G. Rogers, "Squeezing flow of fibre-reinforced viscous fluids," *J. Eng. Math.*, vol. 23, no. 1, pp. 81–89, 1989, doi: 10.1007/BF00058434.

[82] Eco-ease, "PET Technical Handbook." pp. 1–19, 2009. [Online]. Available: https://ecoease.co.uk/wp-content/uploads/2018/09/PET-Technical-Handbook-1.pdf

[83] K. J. Bowles and S. Frimpong, "Void Effects on the Interlaminar Shear Strength of Unidirectional Graphite-Fiber-Reinforced Composites," *J. Compos. Mater.*, vol. 26, no. 10, pp. 1487–1509, 1992, doi: 10.1177/002199839202601006.

[84] K. Chen, M. Jia, H. Sun, and P. Xue, "Thermoplastic reaction injection pultrusion for continuous glass fiber-reinforced polyamide-6 composites," *Materials (Basel).*, vol. 12, no. 3, 2019, doi: 10.3390/ma12030463.

[85] Y. C. Chiou, M. Y. Shen, C. L. Chiang, Y. L. Li, and W. M. Lai, "Effects of Environmental Aging on the Durability of Wood-Flour Filled Recycled PET/PA6 Wood Plastic Composites," *J. Polym. Environ.*, vol. 30, no. 4, pp. 1300–1313, 2022, doi: 10.1007/s10924-021-02268-2.

[86] J. P. Greene, "Engineering Plastics," in *Plastics Design Library, Automotive Plastics and Composites*, J. P. Greene, Ed. William Andrew Publishing, 2021, pp. 107–125. doi: https://doi.org/10.1016/B978-0-12-818008-2.00022-2.

[87] N. M. L. Mondadori, R. C. R. Nunes, L. B. Canto, and A. J. Zattera, "Composites of recycled PET reinforced with short glass fiber," *J. Thermoplast. Compos. Mater.*, vol. 25, no. 6, pp. 747–764, 2012, doi: 10.1177/0892705711412816.

[88] A. strength in Materials, “933 S-2 Glass Yarn.” AGY strength in materilas, United States, p. 2, 2013.

[89] K. Molnár, E. Košťáková, and L. Mészáros, “The effect of needleless electrospun nanofibrous interleaves on mechanical properties of carbon fabrics/epoxy laminates,” *Express Polym. Lett.*, vol. 8, no. 1, pp. 62–72, 2014, doi: 10.3144/expresspolymlett.2014.8.

APPENDIX A THERMAL PROPERTIES OF PET

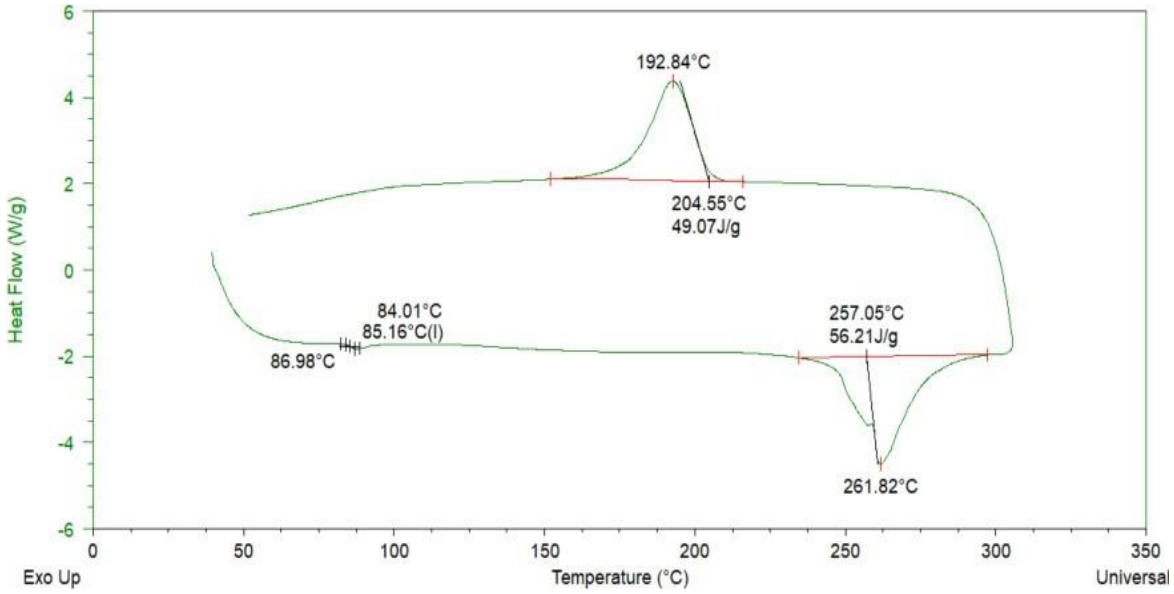

Figure A 1 MDSC thermograms obtained for PET used in the fabrication of GF/PET DREF yarns

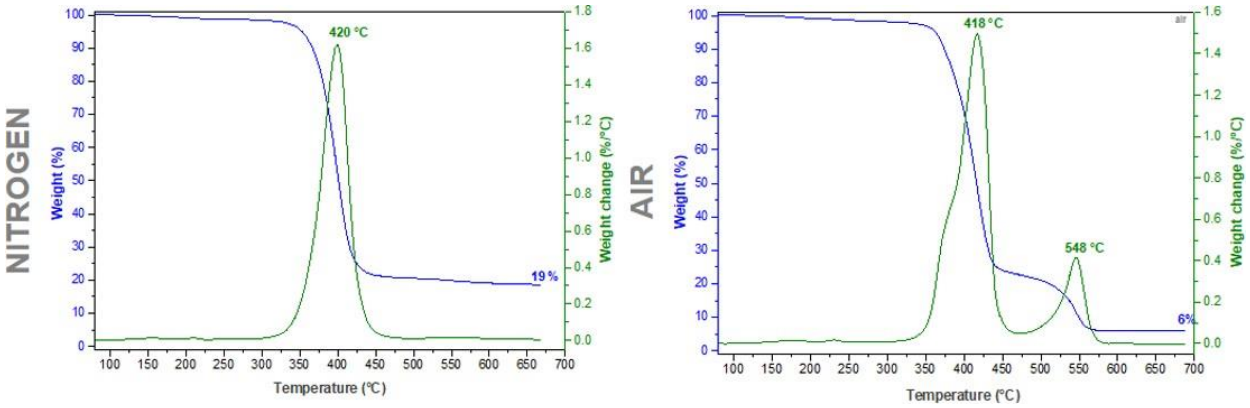

Figure A 2 TGA thermograms in nitrogen and air obtained for PET used in the fabrication of GF/PET DREF yarns

APPENDIX B CONSOLIDATED LAMINATES

Table A 1. Consolidated laminates: (a)-(b) M1P3T3, (c)-(d) M2P3T1, (e)-(f) M1P1T1, (g)-(h) M2P1T2, (i)-(j) M1P2T2, (k)-(l) M2P2T3

(a)

(b)

(c)

(d)

(e)

(f)

(g)

(h)

(i)

(j)

(k)

(l)

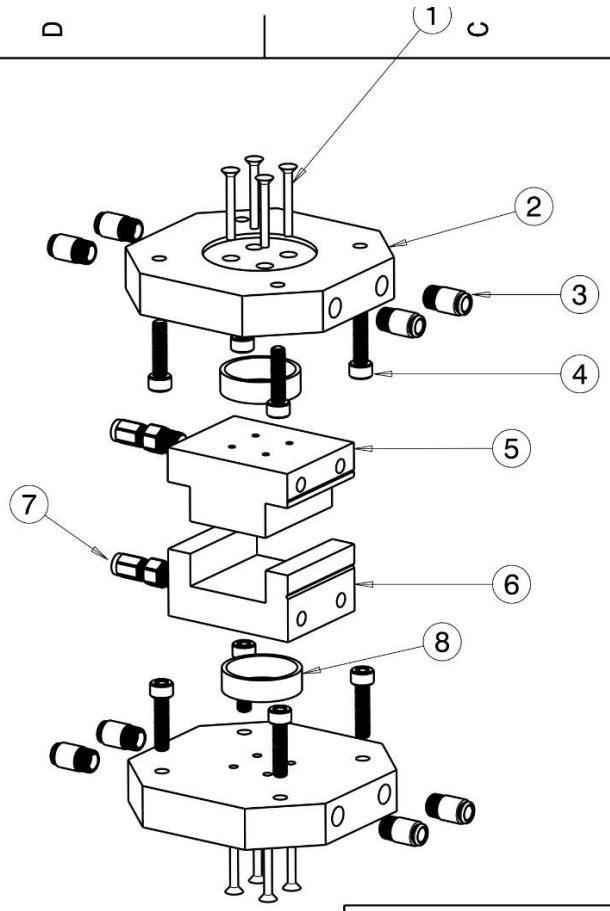

No	Qty	Name	Page
1	8	Interface to tool screw	See BOM
2	2	Interface Load Cell	2
3	8	Cooling tube fitting	See BOM
4	8	Load Cell Screw	See BOM
5	1	Male Tool	3
6	1	Female Tool	4
7	2	Thermocouple Fitting	See BOM
8	2	Thermal Barrier Spacer	5

LABSFCA
ACFSLAB

DESSINÉ PAR: L LABERGE LEBEL	DATE: 2021-07-19	TITRE DU DESSIN: Acumen 12 Material Tooling Assy			
VÉRIFIÉ PAR: L LABERGE LEBEL	DATE: 2021-07-19	FORMAT: A	NUMÉRO DE DESSIN: ACFS-004-001		RÉV: B
RÉVISÉ PAR: L LABERGE LEBEL	DATE: 2021-08-24	ÉCHELLE: 2:5	MASSE(kg): N/A		PAGE: 1/5

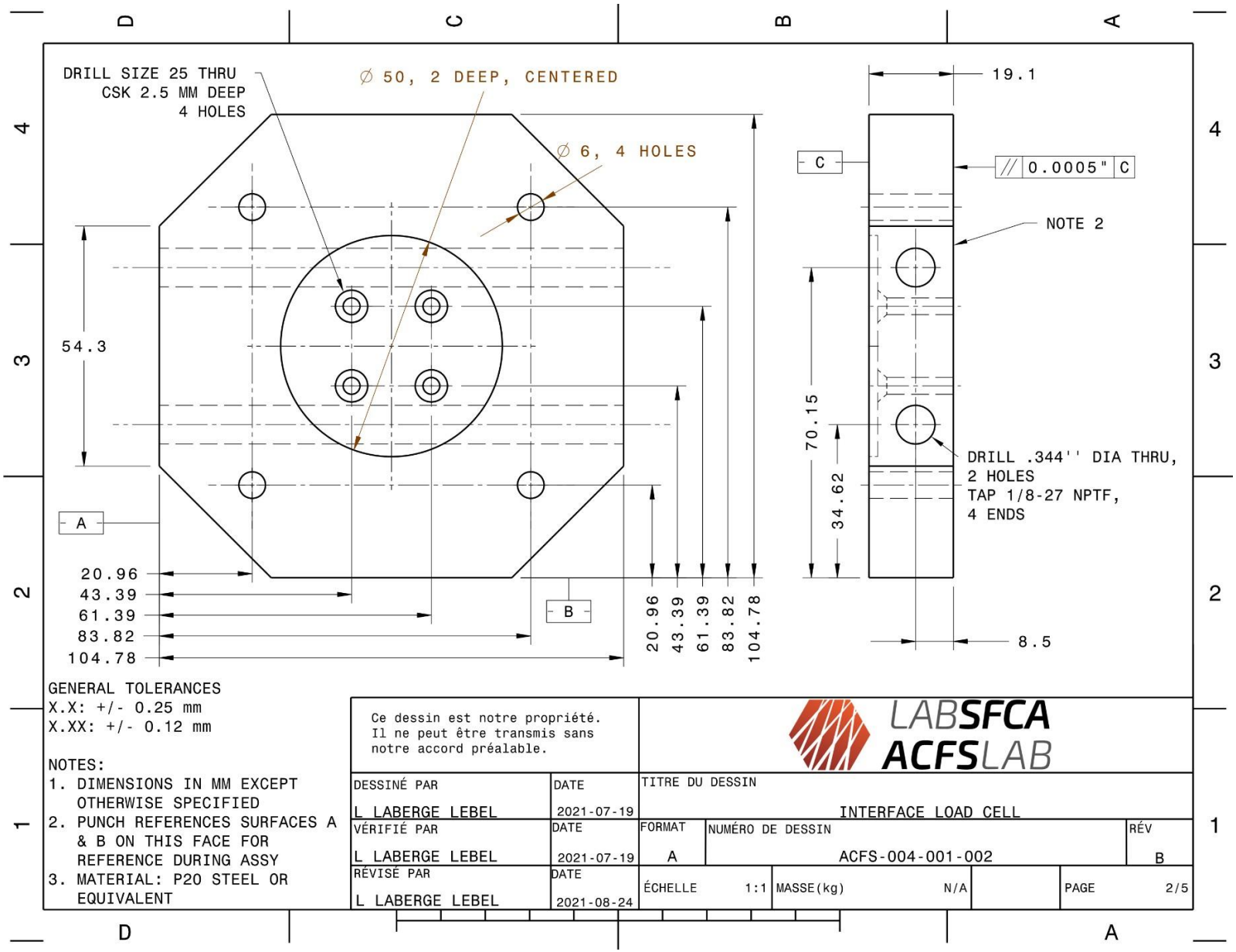

GENERAL TOLERANCES
X.X: +/- 0.25 mm
X.XX: +/- 0.12 mm

NOTES:
1. DIMENSIONS IN MM EXCEPT OTHERWISE SPECIFIED
2. PUNCH REFERENCES SURFACES A & B ON THIS FACE FOR REFERENCE DURING ASSY
3. MATERIAL: P20 STEEL OR EQUIVALENT

LABSFCA
ACFSLAB

DESSINÉ PAR: L LABERGE LEBEL	DATE: 2021-07-19	TITRE DU DESSIN: INTERFACE LOAD CELL	
VÉRIFIÉ PAR: L LABERGE LEBEL	DATE: 2021-07-19	FORMAT: A	NUMÉRO DE DESSIN: ACFS-004-001-002 — RÉV: B
RÉVISÉ PAR: L LABERGE LEBEL	DATE: 2021-08-24	ÉCHELLE: 1:1	MASSE(kg): N/A — PAGE: 2/5

GENERAL TOLERANCES
X.X: +/- 0.25 mm
X.XX: +/- 0.12 mm

MATERIAL: P20 STEEL OR EQUIVALENT

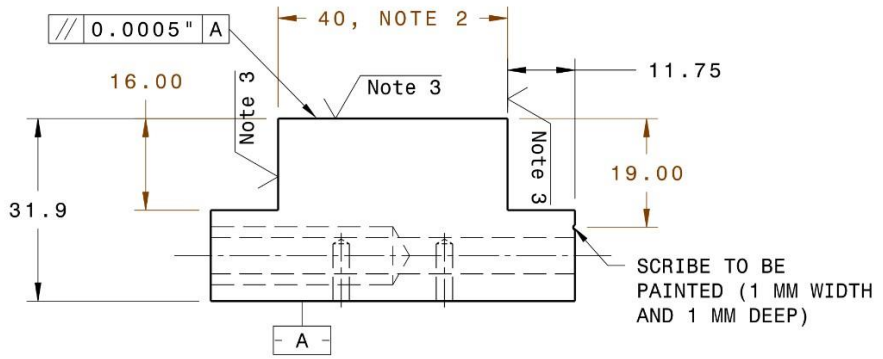

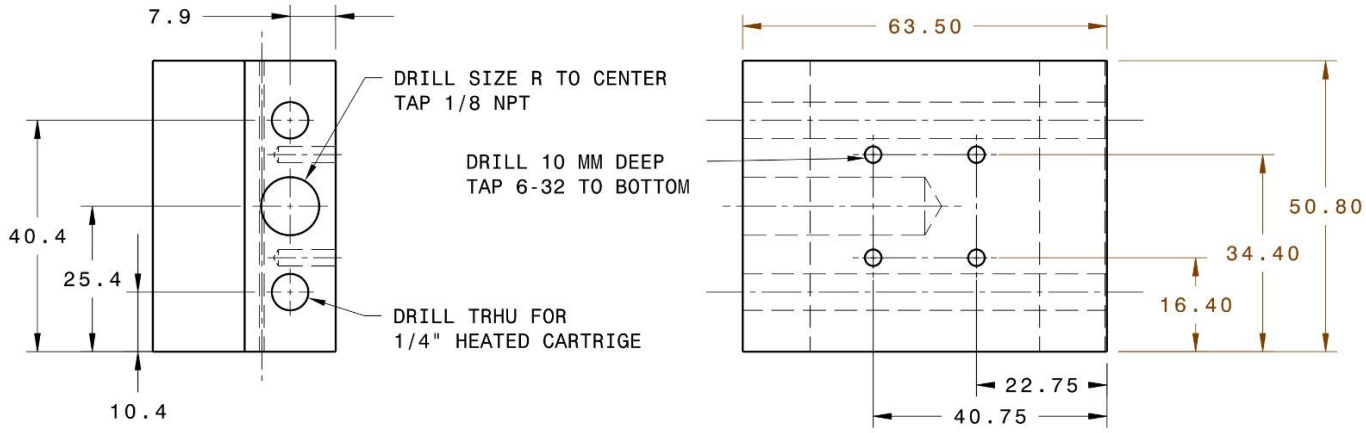

NOTES:
1. DIMENSIONS IN MM EXCEPT OTHERWISE SPECIFIED
2. INSURE ANSI RC3 FIT WITH FEMALE TOOL, CLEARANCE OF 0.0010" TO 0.0026", CONSIDER NOTE 3
3. POLISH SPI A-2 FINISH AND CHROME

LABSFCA
ACFSLAB

DESSINÉ PAR: L LABERGE LEBEL	DATE: 2021-07-19	TITRE DU DESSIN: MALE TOOL			
VÉRIFIÉ PAR: L LABERGE LEBEL	DATE: 2021-07-19	FORMAT: A	NUMÉRO DE DESSIN: ACFS-004-001-005		RÉV: B
RÉVISÉ PAR: L Laberge Lebel	DATE: 2021-08-24	ÉCHELLE: 1:1	MASSE(kg): N/A		PAGE: 3/5

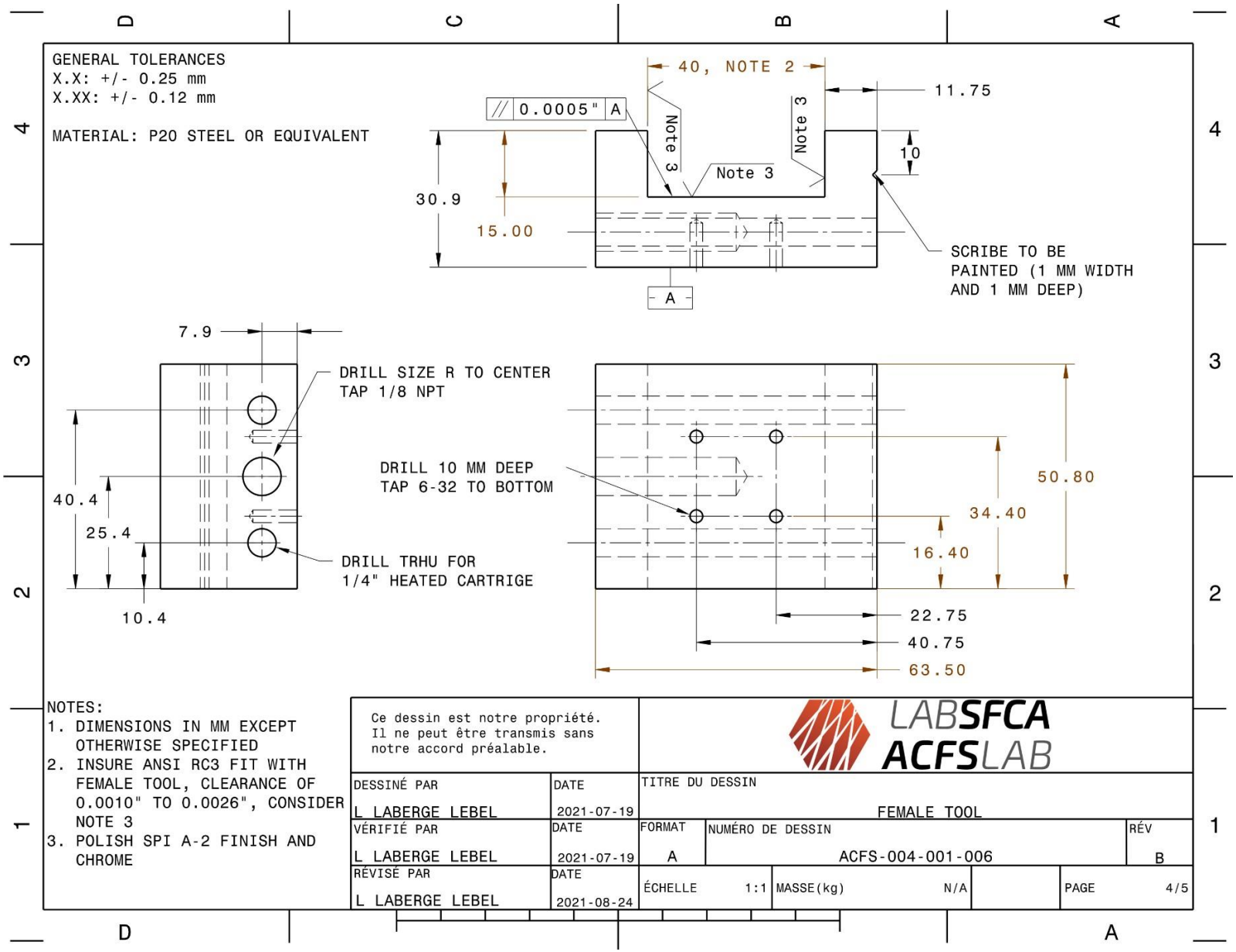
GENERAL TOLERANCES
X.X: +/- 0.25 mm
X.XX: +/- 0.12 mm
MATERIAL: P20 STEEL OR EQUIVALENT
40, NOTE 2
11.75
0.0005" A
Note 3
Note 3
Note 3
10
30.9
15.00
A
SCRIBE TO BE PAINTED (1 MM WIDTH AND 1 MM DEEP)
7.9
DRILL SIZE R TO CENTER TAP 1/8 NPT
DRILL 10 MM DEEP TAP 6-32 TO BOTTOM
DRILL TRHU FOR 1/4" HEATED CARTRIGE
40.4
25.4
10.4
50.80
34.40
16.40
22.75
40.75
63.50
NOTES:
1. DIMENSIONS IN MM EXCEPT OTHERWISE SPECIFIED
2. INSURE ANSI RC3 FIT WITH FEMALE TOOL, CLEARANCE OF 0.0010" TO 0.0026", CONSIDER NOTE 3
3. POLISH SPI A-2 FINISH AND CHROME
Ce dessin est notre propriété. Il ne peut être transmis sans notre accord préalable.
LABSFCA
ACFSLAB
DESSINÉ PAR
L LABERGE LEBEL
DATE
2021-07-19
TITRE DU DESSIN
FEMALE TOOL
VÉRIFIÉ PAR
L LABERGE LEBEL
DATE
2021-07-19
FORMAT
A
NUMÉRO DE DESSIN
ACFS-004-001-006
RÉV
B
RÉVISÉ PAR
L LABERGE LEBEL
DATE
2021-08-24
ÉCHELLE
1:1
MASSE(kg)
N/A
PAGE
4/5

GENERAL TOLERANCES
X.X: +/- 0.25 mm
X.XX: +/- 0.12 mm

MATERIAL: STAINLESS STEEL

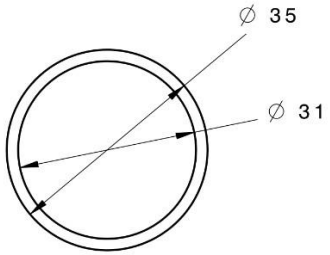

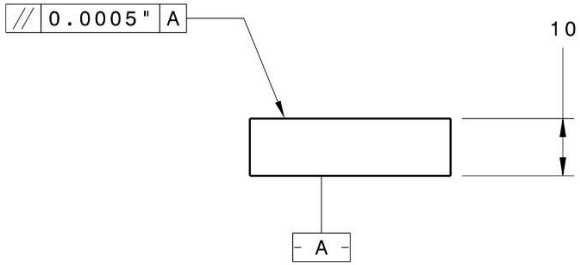

NOTES:
1. DIMENSIONS IN MM EXCEPT OTHERWISE SPECIFIED

LABSFCA
ACFSLAB

DESSINÉ PAR: L LABERGE LEBEL	DATE: 2021-07-19	TITRE DU DESSIN: THERMAL BARRIER SPACER			
VÉRIFIÉ PAR: L LABERGE LEBEL	DATE: 2021-07-19	FORMAT: A	NUMÉRO DE DESSIN: ACFS-004-001-008		RÉV: B
RÉVISÉ PAR: L LABERGE LEBEL	DATE: 2021-08-24	ÉCHELLE: 1:1	MASSE(kg): N/A		PAGE: 5/5